

Regulation of VEGF by TEAD4 and HIF-1 α in Murine Oxygen-Induced Retinopathy

By

Robert S. Cargill

A Dissertation in partial fulfillment of the requirements for the degree of
Doctor of Philosophy

Presented to the Neuroscience Graduate Program

OREGON HEALTH & SCIENCE UNIVERSITY


School of Medicine

May 2013

School of Medicine
Oregon Health & Science University

CERTIFICATE OF APPROVAL

This is to certify that the Ph.D. dissertation of
ROBERT CARGILL
has been approved on May 24, 2013




Advisor, Timothy Stout, M.D., Ph.D., M.B.A.



Member and Chair, Catherine Morgans, Ph.D.



Member, Gary Westbrook, M.D.



Member, Zheng David Qian, Ph.D.

TABLE OF CONTENTS

Chapter I. BACKGROUND AND INTRODUCTION	2
NEOVASCULAR RETINOPATHIES	4
OXYGEN-INDUCED RETINOPATHY ANIMAL MODELS	5
VEGF	8
HYPOXIA-INDUCIBLE FACTOR.....	10
MÜLLER GLIA AND RETINAL STRUCTURE	12
TEAD4 IN HYPOXIA AND OCULAR DISEASE.....	13
TEAD FAMILY TRANSCRIPTION FACTORS	16
TEAD4 REGULATION OF HIF-1 α	19
Chapter II. TEAD4 AND VEGF IN AN OXYGEN-INDUCED RETINOPATHY MOUSE	
MODEL OF NEOVASCULAR DISEASE	22
INTRODUCTION	24
RESULTS	25
DISCUSSION	29
MATERIALS AND METHODS	31
Chapter III. EFFECT OF TEAD4 OVEREXPRESSION ON VEGF PROMOTER	
ACTIVITY <i>IN VITRO</i>	34
INTRODUCTION	36
RESULTS	38
DISCUSSION	48
MATERIALS AND METHODS	52
SUPPLEMENTAL METHODS	54

Chapter IV. TEAD4 INCREASES VEGF PROMOTER ACTIVITY WITHIN A MÜLLER GLIAL CELL LINE INDIRECTLY THROUGH HIF-1 α	60
INTRODUCTION	62
RESULTS	64
DISCUSSION	74
MATERIALS AND METHODS	77
Chapter V. SUMMARY AND CONCLUSIONS	82

LIST OF FIGURES

Figure I.1. Neovascularization in the P17 OIR retina.	6
Figure I.2. Immunohistochemical staining using polyclonal anti-VEGF/VPF antibodies in OIR retina.....	7
Figure I.3. VEGFA Gene Structure and Splice Variants	9
Figure I.4. Regulation of Hypoxia Inducible Factor-1.....	10
Figure I.5. Golgi-stained Müller glia from various species (from Bringmann and Cajal)	12
Figure I.6. Müller cell functions in the retina (from Bringmann 2006)	13
Figure I.7. Exon Structure of TEAD4 Isoform transcripts.....	15
Figure II.1. TEAD4 and VEGF expression patterns over the course of development and OIR progression	27
Figure II.2. Four unique TEAD4 transcripts identified within murine retinas	28
Figure III.1. Comparison of mouse vs. human VEGF promoter activation by murine TEAD4.	43
Figure III.2. TEAD4 and VEGF expression <i>in vitro</i>	44
Figure III.3. Fluorescence microscopy images from optimization of Amaxa nucleofection in MIO-M1.	45
Figure III.4. VEGF promoter activity following TEAD4 overexpression.....	46
Figure III.5. Effect of TEAD4 overexpression on native VEGF expression levels.....	47
Figure III.6. Generation of plasmids for reporter assays.....	58
Figure III.7. Human and mouse VEGF promoter sequence showing primer locations vs. HRE, MCAT, and Sp1 sites.....	58
Figure IV.1. Effect of HIF-1 α inhibition by YC-1 on VEGF promoter activity in hypoxic MIO-M1 cells.....	68

Figure IV.2. <i>Vegf</i> promoter activity in a HIF-1-deficient cell line.	69
Figure IV.3. siRNA knockdown of HIF-1 α in MIO-M1 cells.	70
Figure IV.4. siRNA knockdown of TEAD4 in MIO-M1 cells.	71
Figure IV.5. Quantitative RT-PCR in MIO-M1 cells treated with TEAD4 and HIF-1 α siRNA.....	72
Figure IV.6. . TEAD4 and GLAST immunostaining of P17 mouse neural retina.....	73

LIST OF ABBREVIATIONS

AMD – age-related macular degeneration

BAEC – bovine aortic endothelial cells

DR – diabetic retinopathy

EC – endothelial cell

GLAST – glutamate aspartate transporter

HIF – hypoxia-inducible factor

HMEC – human microvascular endothelial cell

HUVEC – human umbilical vein endothelial cell

IHC – immunohistochemistry

MCAT – muscle-specific cytosine/adenine/thymine (CAT) sequence

NV – neovascularization

OIR – oxygen-induced retinopathy

PCR – polymerase chain reaction

qPCR – quantitative PCR

ROP – retinopathy of prematurity

RT-PCR – reverse transcription PCR

SEAP – secretable alkaline phosphatase

siRNA – small interfering ribonucleic acid

TEAD – TEF/TEC/ABAA DNA binding domain

TEF – transcriptional enhancer factor

VEGF – vascular endothelial growth factor

ACKNOWLEDGEMENTS

I owe a great deal of thanks to both of my mentors, Binoy Appukuttan and Tim Stout, without whose direction and financial support, I would have never found my way to completion.

This dissertation could not have been possible without the outstanding support of my labmates, Trevor McFarland, Matt Hartzell, and Andrew Stempel. Thank you for all the technical support and direction, for all the times you repeated yourself for my benefit, and for putting up with me as I slogged through this phase of my life! I'll clean up, I promise! I also received significant encouragement and advice from Ted Acott and Catherine Morgans.

The OIR mice used were the work of the skilled lab of Mike Powers, Mike Davies, and Andrew Stempel. I am very thankful for the raw materials for my studies. The C57M10 cell line was a generous gift of Deb Otteson, University of Houston. MIO-M1 cells were a gift of Astrid Limb at the Institute of Ophthalmology and Moorfields Eye Hospital, London, United Kingdom.

I also owe thanks to the National Eye Institute, the source of my funding through the following grants: NIH:NEI:R01 EY019042 and NIH:NEI:R01 EY011548. Additional funding was provided by Research to Prevent Blindness

Finally, I owe my family a huge thank you for putting up with me as I explored this phase of my development. This work is dedicated to my children, Aaron and Norah Cargill, who have had to share their father with The Lab; my mother Barbara Cargill, whose years of sacrifice helped me to unlock the potential that life has to offer; and my father, Steve Cargill, my role model and source of constant moral support.

ABSTRACT

Retinopathies comprise a group of non-inflammatory diseases of the retina, including diabetic retinopathy, age-related macular degeneration, and retinopathy of prematurity. These disorders impact nearly ten million people in the United States, representing the leading cause of blindness. The pathogenesis of neovascular retinopathies has been studied intensively in animal models, including a widely used mouse model of oxygen-induced retinopathy pioneered by Lois Smith.¹¹ Vascular endothelial growth factor, produced by Müller glia in response to hypoxia, is a potent mitogen responsible for formation of vision-destroying neovascular growths, and anti-VEGF treatments are now the standard of care for treatment of most neovascular ocular diseases. However, there remains intense interest in novel strategies for treatment of neovascular disease within academia and industry.

The canonical regulatory pathway for VEGF is through Hypoxia Inducible Factor. However, more recent data from bovine aortic endothelial cells³⁴ revealed a novel regulator for VEGF: TEAD4, a member of the transcription enhancer factor family. Subsequent investigations at the Casey Eye Institute have shown that TEAD4 is present in primate ocular cells.^{35 36} We report here that TEAD4 as well VEGF is upregulated during the neovascular phase of murine OIR. Using cell lines with Müller glia-like properties *in vitro*, we found that TEAD4 activates both the mouse and human VEGF promoter despite differences in critical promoter sequences. TEAD4 increased VEGF promoter activity further under hypoxia, suggesting it is involved in hypoxic induction of the gene. However, the effect appeared to be mediated indirectly through its ability to influence *HIF1 α* transcription. Finally, immunohistochemical staining

indicated that TEAD4 is expressed in endothelial cells of neovascular tufts within the OIR retina, suggesting future studies on the involvement of TEAD4 in regulation of HIF-1 in retinal vascular endothelial cells.

Chapter I.

BACKGROUND AND INTRODUCTION

- A. NEOVASCULAR RETINOPATHIES
- B. OXYGEN-INDUCED RETINOPATHY ANIMAL MODELS
- C. VEGF
- D. HYPOXIA-INDUCIBLE FACTOR
- E. MÜLLER GLIA AND RETINAL STRUCTURE
- F. TEAD4 IN HYPOXIA AND OCULAR DISEASE
- G. TEAD FAMILY TRANSCRIPTION FACTORS

NEOVASCULAR RETINOPATHIES

Retinopathy is the name given to any one of a number of noninflammatory diseases of the retina, typically classified according to their pathophysiology. Many retinopathies are proliferative in nature, characterized by neovascularization (NV), the abnormal growth of blood vessels on the surface of the retina. Several ocular diseases have one or more forms that involve NV, including diabetic retinopathy (DR), age-related macular degeneration (AMD), and retinopathy of prematurity (ROP). As a group, these three angiogenic ocular diseases represent the leading cause of vision loss in the developed world.¹

DR is a complication of diabetes mellitus, affecting nearly half of all patients with Type I or Type II diabetes. The longer a person lives with diabetic symptoms, the more likely they are to face this common complication. It begins as a microvascular pathology resulting from the chronic hyperglycemia of diabetes, which causes pericyte apoptosis and compromises the retinal vascular network. Ocular hemorrhage and regional hypoxia result, producing spots or blurring in the field of vision. The disease frequently progresses to proliferative DR, characterized by hypoxia-induced production of growth factors and angiogenesis of leaky neovascular processes.

AMD refers to a group of diseases that result in loss of acuity in the center of the field of vision. In the wet, or exudative, form of the disease, abnormal blood vessel growth occurs at the outside of the retina, between the retina and choroid. Although this represents only a small fraction of total cases, they include the vast majority with severe vision loss. While the mechanism remains under investigation, it appears that oxidative stress and dysregulation of the complement system within Bruch's membrane may be involved in triggering excessive growth factor production.¹

Retinopathy of Prematurity (ROP) is a disease that affects over 65% of premature infants having birth weight below 1.25kg,² and is the leading cause of preventable childhood blindness in the United States.³ In ROP, supplemental oxygen treatment administered to support on-going fetal development *ex utero* increases oxygen saturation levels from 80% normally found in the late-term fetus to over 95%, causing retinal hyperoxia and aborting normal vasculogenesis.⁴ Without normal vascular development, retinal oxygen demand soon outstrips that supplied by the vasculature, leading to a hypoxic condition that frequently induces neovascularization of the retina. ROP first appeared as supplemental oxygen treatment came into use in neonatal care, then abated as supplemental oxygen use was restricted as a response to the appearance of the disease. However, severe complications in mental development led to a resumption of oxygen use and consequent increases in ROP. Traditional treatments included laser photocoagulation to reduce retinal bleeding. More recently, anti-VEGF treatments such as bevacizumab have come into use, providing more reliable relief from the effects of the disease.⁵ However, there remain concerns about the long-term safety and efficacy of the treatment as VEGF is known to provide neurotrophic support within the retina.^{6 7}

OXYGEN-INDUCED RETINOPATHY ANIMAL MODELS

Several models of retinopathy have been developed in animals including mice, rats, cats, dogs, and non-human primates. Most involve vaso-obliterative treatments that either restrict perfusion to a region of the retina or abort normal developmental vasculogenesis by hyperoxic exposure as in the human ROP disease. The occlusive strategies can be implemented by surgical obstruction, elevation of intraocular pressure, or by laser-induced photocoagulation. The latter oxygen-induced approaches can be implemented in several species by maintaining the developing neonate of the species in a hyperoxic environment

during a critical window of retinal vasculogenesis. The earliest such studies were carried out by Ashton using rats,⁸ with similar studies using rabbits,⁹ puppies, and kittens¹⁰ to follow.

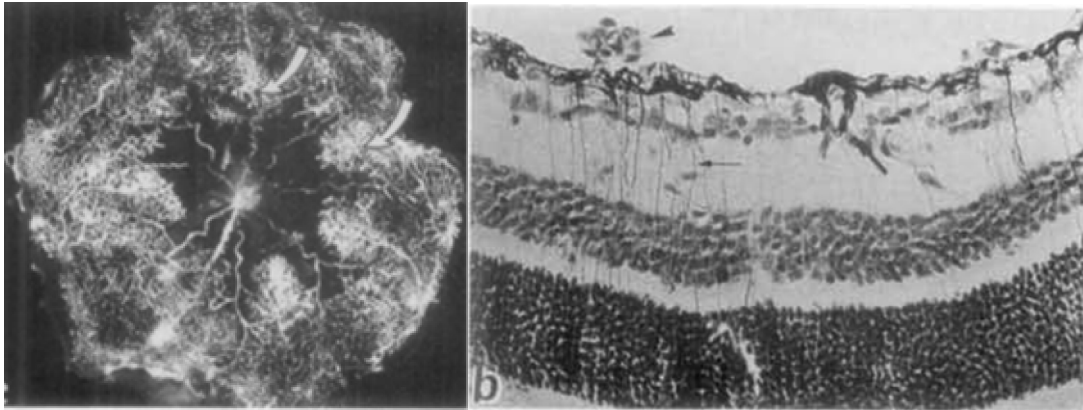


Figure I.1. Neovascularization in the P17 OIR retina. (from Smith, 1994¹¹) Left: fluorescein angiography in retinal flat mount showing central avascular area surrounded by brightly-labeled NV tufts (arrows) at the boundary between the vascular and avascular regions. Right: P17 cross-section immunostained for GFAP showing neovascular tuft (arrowhead).

In 1994, Lois Smith published a protocol for oxygen-induced retinopathy (OIR) in the mouse,¹¹ which is now one of the most widely used models of ROP. In this model, C57BL6 pups with their nursing mothers are transferred to 75% oxygen at post-natal day 7 (P7), and maintained there until P12, when they are returned to room air. The resulting elevation in blood oxygen tension at P7 drives a rapid vaso-obliteration during what is normally the most active period of vasculogenesis within the murine retina. The return to room air causes an acute hypoxia within the inadequately vascularized retina, resulting in a rapid and repeatable neovascular response. Treated retinas exhibit extensive formation of endothelial-rich preretinal tufts, largely at the boundary between the avascular central retina and the normally-vascularized periphery (Figure I.1). The severity of NV peaks at P17, with a gradual regression over the course of the following week. By P24, there is little difference between the treated animals and room-air controls.

The pathomechanism of OIR has been widely investigated and involves the rapid onset of VEGF production by Müller glia within the first day of return to room air (Figure I.2). VEGF is one of a multitude of hypoxia-responsive genes containing the HIF-1-binding Hypoxia Response Element (HRE). HIF-1 α , stabilized due to the lack of oxygen within the poorly vascularized retina, binds to the VEGF promoter, driving increased synthesis and secretion. VEGF acts in paracrine fashion by binding to receptors expressed on endothelial cells within the developing vasculature, causing endothelial cell proliferation and migration. The result is uncontrolled blood vessel growth, generating neovascular tufts. At the conclusion of the neovascular phase, the tufts are gradually reabsorbed, and unlike human ROP, vasculogenesis resumes normally. In a classic translational research success story, animal models of retinopathy have proven their utility in the development of several anti-VEGF treatments for human ocular neovascular disease.

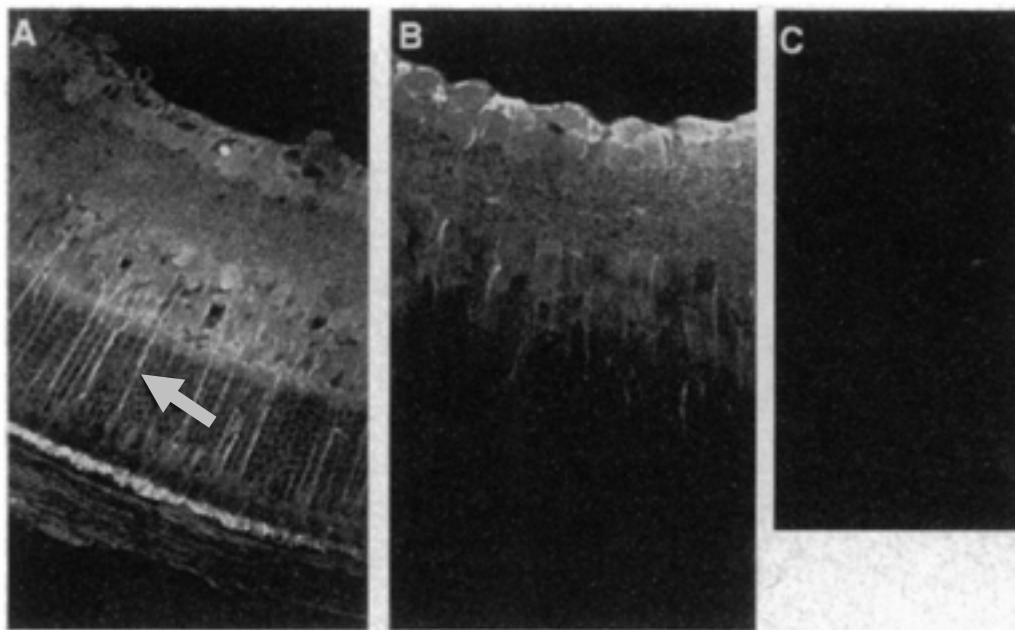


Figure I.2. Immunohistochemical staining using polyclonal anti-VEGF/VPF antibodies in OIR retina. (Pierce et al. 1995¹²) (A) P17 OIR retina. (B) P17 control retina. (C) No primary control. Immunostained radial processes in (A) spanning the retinal thickness are consistent with Müller glial morphology (arrow).

VEGF

The VEGF family consists of five highly conserved proteins (VEGFA, VEGFB, VEGFC, VEGFD, and Placental Growth Factor PLGF) that share a common cysteine knot structure characteristic of the PDGF (Platelet Derived Growth Factor) superfamily. As a group, they modulate endothelial cell proliferation, migration, and differentiation¹³ via signaling through a group of three cell surface receptors, VEGFR1 (Flt-1), VEGFR2 (KDR/Flk-1), and VEGFR3.¹⁴ VEGF receptors contain an extracellular structure comprised of seven immunoglobulin-like domains, which couple to one another to form VEGF-binding homo- or hetero-dimers. Intracellular receptor tyrosine kinase domains become autophosphorylated upon ligand binding, and signal via intracellular messengers including Src and phospholipase C. Whereas VEGFB is involved in vascular homeostasis¹⁵ and lipid uptake by endothelial cells,¹⁶ VEGFC and VEGFD primarily impact lymphangiogenesis.¹⁴

VEGFA, hereafter simply VEGF, is recognized as a critical regulator of developmental vasculogenesis as well as angiogenesis, the formation of new blood vessels from the existing vasculature. VEGFA has been studied intensively following discovery of its pivotal role in vasculogenesis and angiogenesis, and is a therapeutic target in human diseases including solid tumor cancers and ocular diseases. Its upregulation under low oxygen conditions is known to be driven by the induction of Hypoxia Inducible Factor-1 (HIF-1).¹⁷ The VEGF gene is comprised of eight exons that are subject to several variations of alternative splicing resulting in proteins with 121, 145, 165, 189, and 206 amino acids,¹⁸ with the 165aa isoform being the most abundant (See Figure I.3). The murine isoforms have similar structure, although they have one fewer amino acid in exon 2. Although the shortest isoform is freely diffusible, the 165aa and longer isoforms have a heparin-binding domain that anchors them to the extracellular matrix.¹⁴ Binding of VEGF to VEGFR2

causes endothelial cell proliferation, migration, and survival, while increasing vascular permeability.

VEGF transcription is regulated by a number of transcription factors, with several consensus binding sites located within the proximal 5' promoter of the gene. Four AP-1 and two AP-2 consensus binding sites are present, as well as NFκB and Sp-1 sites.^{18 19 20} There is also an HRE, the binding site for HIF-1, located 975 nucleotides upstream of the transcription initiation site. Additional elements within the 5' UTR, coding region, and 3' UTR also participate in post-transcriptional regulation,²¹ adding to the complexity of VEGF gene regulation.

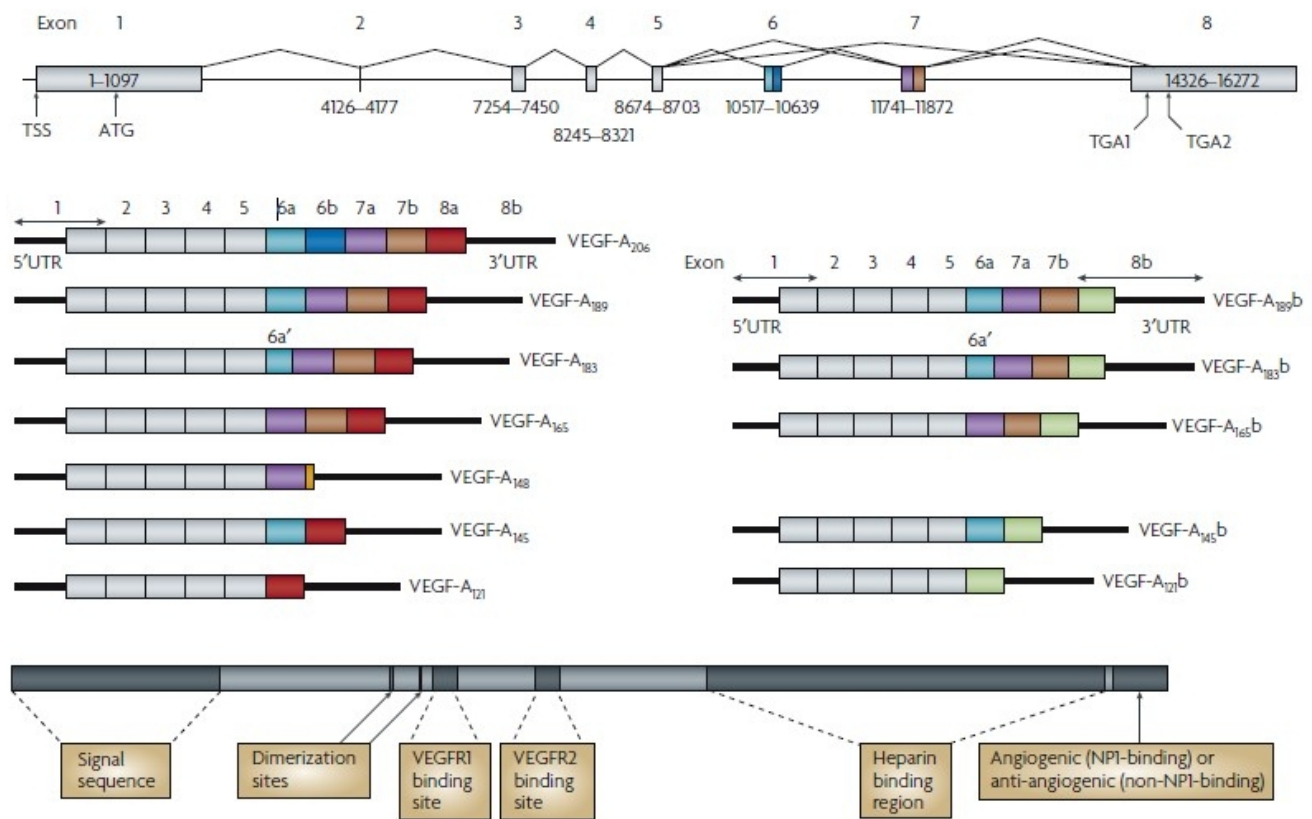


Figure I.3. VEGFA Gene Structure and Splice Variants
(reproduced from Harper and Bates,²² Copyright Nature Publications, 2005.)

HYPOXIA-INDUCIBLE FACTOR

Adaptive responses to variation in oxygen levels are critical to the survival of any aerobic organism, so it should come as no surprise that evolution has delivered a well-developed system of responding to changes in availability of oxygen. Probably the best

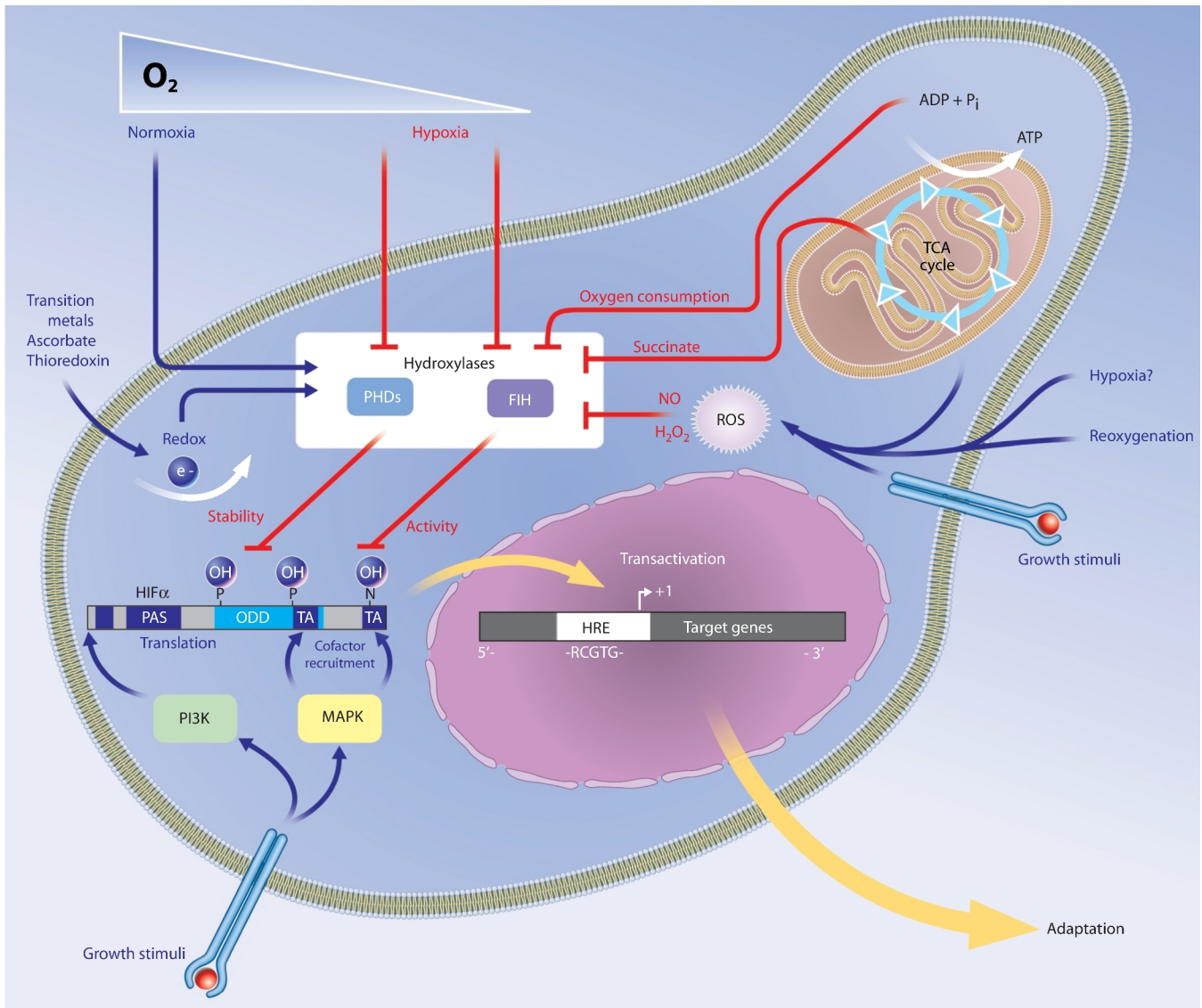


Figure I.4. Regulation of Hypoxia Inducible Factor-1
(reproduced from Wenger et al. *STKE*. 2005²⁵)

characterized pathway for response to acute oxygen deprivation is the one regulated by Hypoxia Inducible Factor 1 (HIF-1, Figure I.4).²⁴ HIF-1 is a heterodimeric basic helix-loop-helix (bHLH) transcription factor comprised of a constitutively expressed HIF-1β subunit

and an oxygen-dependent HIF-1 α subunit. The alpha subunit is subject to rapid turnover under normoxic conditions, synthesized continuously but rapidly degraded.²⁵ As depicted in the white box in the center of the figure, this process is controlled by a group of oxygen-dependent Factors Inhibiting HIF (FIH) and Prolyl Hydroxylases (PHDs) that hydroxylate HIF-1 α multiple proline residues within its oxygen-dependent degradation domain (ODD). This encourages binding of von Hippel-Lindau (VHL) tumor suppressor protein, which targets the protein for proteasomal degradation.²⁶ Because the hydroxylase activity depends upon a non-heme ferric catalytic site whose activity requires the presence of oxygen, it is unable to act on HIF-1 α under hypoxic conditions, blocking its degradation and causing the rapid accumulation of the protein.²⁷ HIF-1 α binds to its beta partner, translocates to the nucleus, and initiates transcription of many hypoxia-responsive genes. HIF-1 forms a complex with p300/CBP and CREB, leading to transcription of genes including VEGF and Epo.²⁸ The consensus sequence RCGTG, where R is either purine base, has been labeled the hypoxia response element (HRE) and has been found in over 200 hypoxia-responsive genes.²⁵

MÜLLER GLIA AND RETINAL STRUCTURE

Müller glia, the cell population identified by Lois Smith as the source of VEGF in the OIR model, are the primary support cells of the retina. They provide critical metabolic support to the spectrum of retinal neurons by maintaining ionic homeostasis, balancing pH, and stabilizing potassium concentrations. They also deliver metabolic inputs and process waste ammonia and CO₂ from aerobic metabolism in support of adjacent neurons.²⁹ Müller glia are also capable of dedifferentiation in certain contexts and may participate in retinal regeneration in some species.³⁰

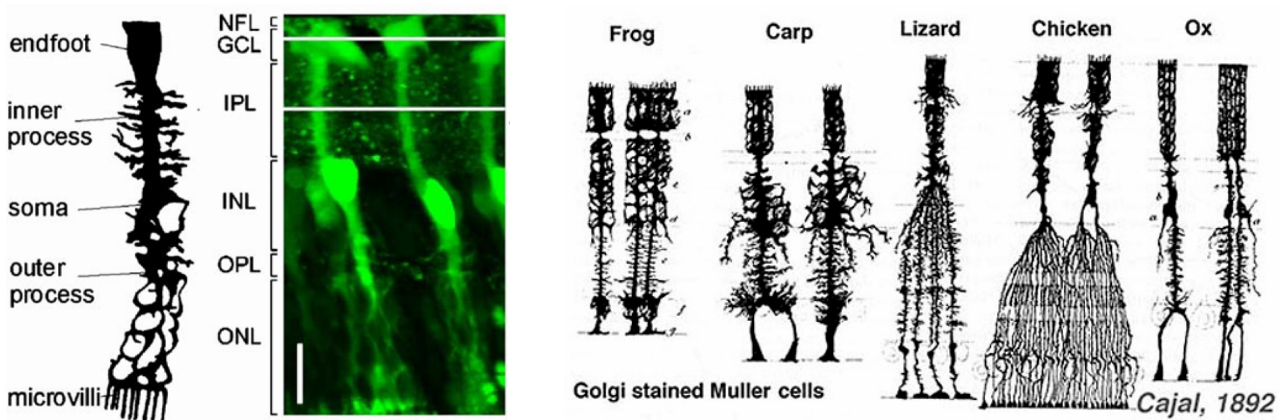


Figure I.5. Golgi-stained Müller glia from various species (from Bringmann²⁹ and Cajal³¹)

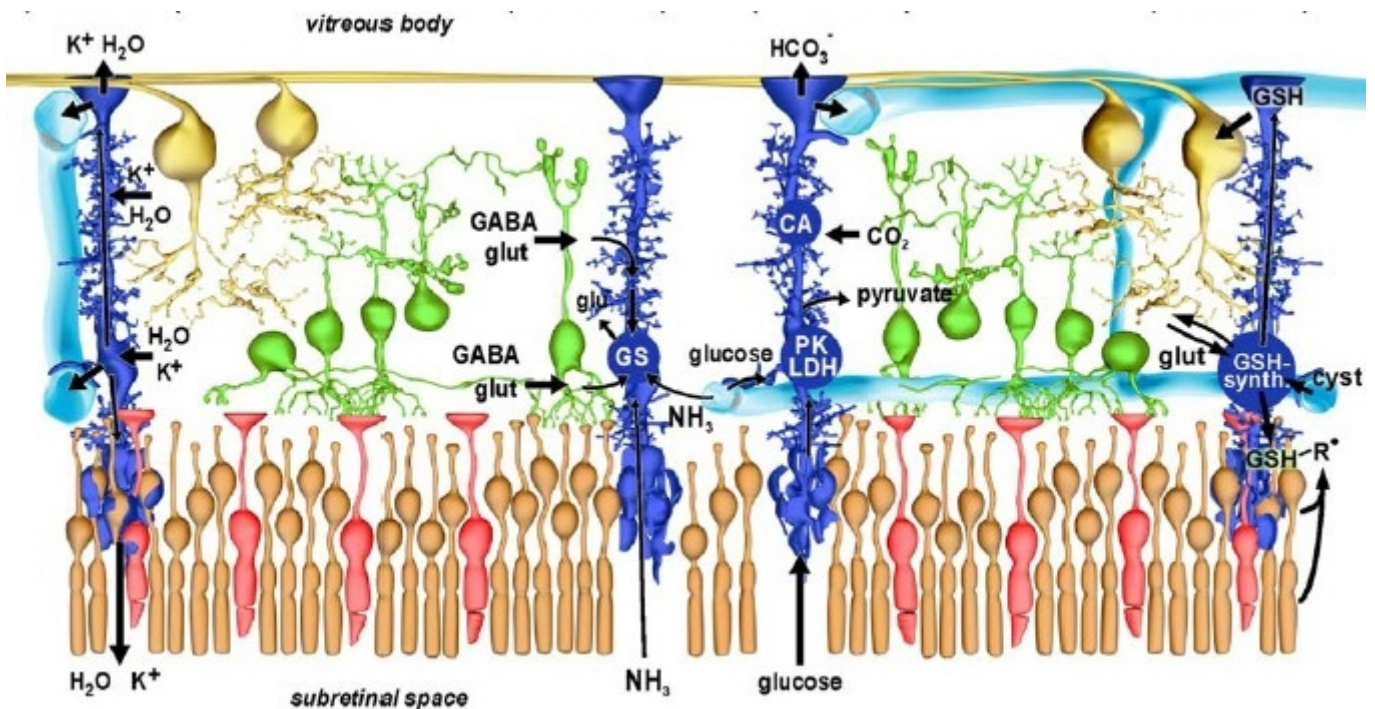


Figure I.6. Müller cell functions in the retina (from Bringmann 2006²⁹)

Spanning the entire depth of the neural retina, Müller glia form the inner limiting membrane with their endfeet, coming in direct contact with the superficial vasculature. They extend processes into the inner plexiform layer (IPL), outer plexiform layer (OPL), and outer nuclear layer (ONL), with nuclei residing in the inner nuclear layer (INL). They sense the condition of all four retinal layers and responding with regulatory feedback to the retinal vasculature. Conditional knockout of either HIF-1 α ³² or VEGF³³ within Müller glia has been shown to cause a substantial lessening of the neovascular response within the mouse OIR model, confirming their importance *in vivo*.

TEAD4 IN HYPOXIA AND OCULAR DISEASE

Whereas the canonical HIF-1 α pathway is widely acknowledged as a key mechanism of control of VEGF expression, a 2004 study from Jian Li's group at Harvard Medical School revealed a novel regulatory factor, TEAD4, found in an unbiased screen for hypoxia-responsive transcription factors within bovine aortic endothelial cells (BAECs).³⁴

Using *VEGF* promoter activity assays, Shie et al. found that TEAD4 bound the first of four Sp1 sites in a GC-rich region of the proximal promoter for the human *VEGF* gene, and its overexpression led to increased levels of expression. Deletion analysis indicated that the first Sp1 site, located 97 nucleotides upstream of the transcription initiation site, was necessary for enhancement of *VEGF* promoter activity. When stably transfected into BAEC, TEAD4 was found to drive a significant increase in proliferation and tube formation in a matrigel assay, suggesting it might play an important role in the transcriptional regulation of *VEGF* under hypoxia.

Because aberrant neovascularization represents a significant pathological mechanism in the case of many different ocular diseases, Appukuttan et al. sought to determine if TEAD4 might be involved in *VEGF* upregulation within the hypoxic eye. TEAD4 was shown to be expressed within the eye, and exhibited alternate splicing in primary human retinal vascular ECs maintained in hypoxic conditions.³⁵ Novel 936bp and 447bp isoforms were found within these cells, and expression patterns varied between control and treated cells. *VEGF* promoter activity assays using cloned versions of the human TEAD4 isoforms demonstrated that the shorter TEAD4₁₄₈ isoform, shown in Figure I.7, was able to enhance promoter activity 10- to 15-fold above background levels. This compared to only three-fold for full-length TEAD4. As shown by the figure, the full-length transcript comprises twelve exons, encoding a protein having 434 amino acids. The 447bp transcript encodes a 148aa protein lacking exon 5 and much of exons 7 to 12, removing the proline rich domain (PRD) and a serine-threonine-tyrosine-rich (STY) domain. However, the nuclear localization signal (NLS) and TEA DNA-binding domain remained intact. Similarly, transcripts for alternate splice variants were found within RNA isolated from neural retina of the P8 and P17 mouse.

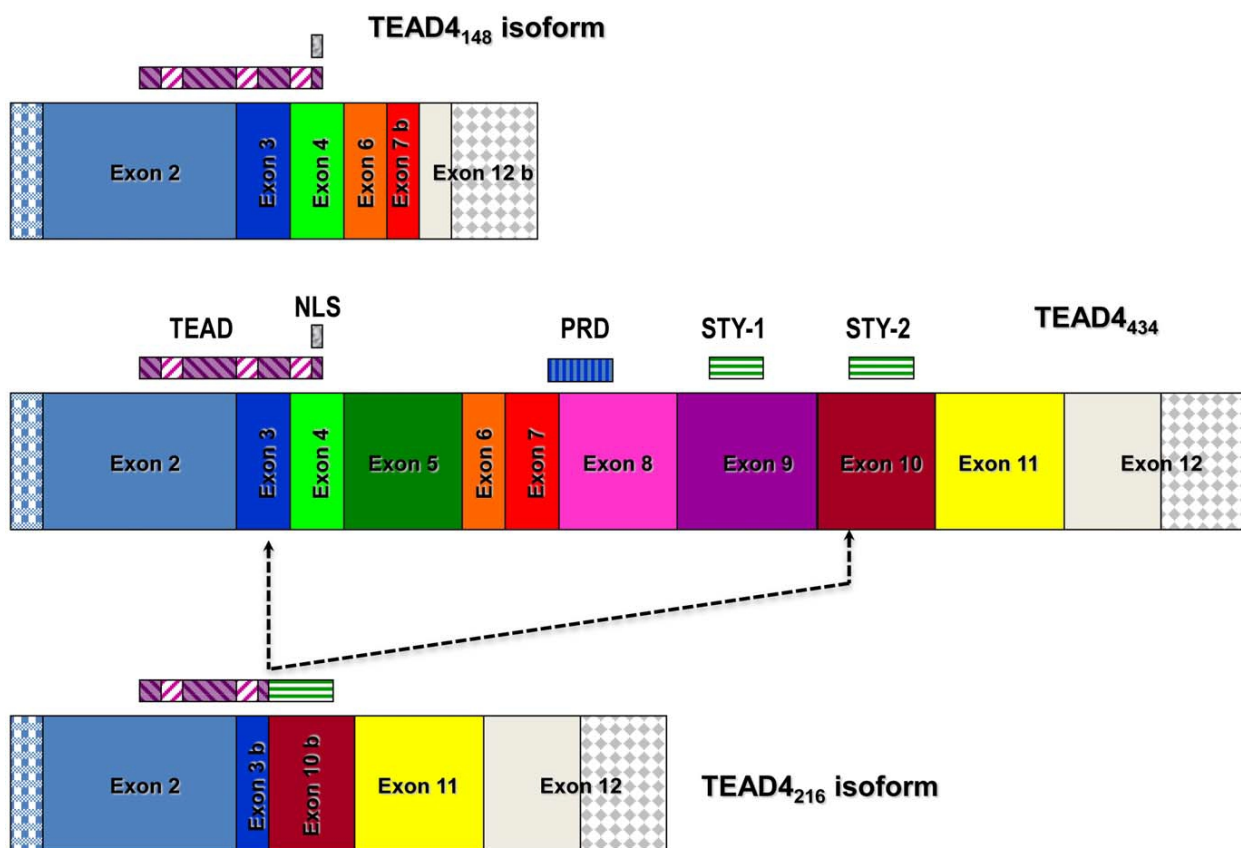


Figure I.7. Exon Structure of TEAD4 Isoform transcripts showing locations of TEA DNA binding domain (TEAD), nuclear localization signal (NLS), proline-rich domain (PRD), and serine-threonine-tyrosine domains (STY). (from Appukuttan et al. PLoS One. 2012;7(6):e31260)

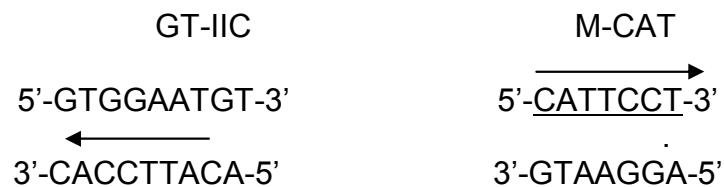
Soon thereafter, Appukuttan *et al.* published the finding of another novel TEAD4 splice variant, TEAD4₂₁₆, found within RNA from primary human retinal endothelial cells.³⁶ This 216aa isoform has an in-frame splicing event that eliminates exons 4 through 9, as well as a portion of exons 3 and 10, as shown in Figure I.7 above. This eliminated the NLS within the TEA DNA-binding domain, the PRD domain, and the first STY domain. TEAD4₂₁₆ was found to inhibit VEGF promoter activity by roughly 50% in gene reporter assays within HEK293T, and was able to competitively inhibit the effect of enhancer isoforms in a dose-dependent manner. This inhibition was maintained in the absence of the HRE, and also under hypoxic conditions. Exogenous expression of the inhibitor isoform reduced VEGF secretion in HEK293T, ARPE-19, and D407 cells, and was found to reduce cellular

proliferation significantly. The inhibitor isoform is unique in that it lacks exon 4 which contains the putative nuclear localization signal. Expression of fluorescently-tagged fusion proteins demonstrated that, in contrast to previously discovered isoforms, TEAD4₂₁₆ is localized to the cytoplasm. In studies using chimeric constructs of TEAD4, it was found that the addition of the NLS to the inhibitor isoform was sufficient for the chimera to gain similar activator function to the other TEAD4 isoforms, whereas removal of the NLS from the enhancer TEAD4₁₄₈ isoform was sufficient to eliminate its activator function. This suggested that cellular localization influenced the activity of the protein.

TEAD FAMILY TRANSCRIPTION FACTORS

TEAD4 is one of four members of the Transcriptional Enhancer Factor family. TEAD1, the first member family of transcription factors, was discovered in 1988 as an abundant DNA binding protein isolated from HeLa cell nuclear extract.³⁷ TEAD1 was found to bind to Sph and GT-IIC motifs from the SV40 enhancer, the latter sharing similarity with muscle-specific CAT (M-CAT) promoter elements shown to be essential for the expression of muscle-specific genes. The founding member of the TEAD family, TEAD1 is the primary transcriptional regulator of several muscle-specific genes including skeletal α -actin (SKA), skeletal troponin T, α -myosin heavy chain, and β -myosin heavy chain.³⁸ TEAD4 was isolated a few years later from human³⁹ and mouse.⁴⁰ Its cloning completed discovery of the family of four mammalian TEADs.⁴¹ TEAD4 shares with the other TEADs a highly conserved TEA DNA binding domain and a C-terminal cofactor interaction domain, but is unique in its capacity for α -adrenergic reactivation of SKA following myocardial infarction.⁴² In 1988, Davidson identified TEF-1, the first of the TEA family of transcription factors, as a 53kDa DNA-binding protein from HeLa cells that bound to the SV40 enhancer.³⁷ TEF-1 was able to bind to both Sph and GT-IIC motifs within the promoter. It was active within

both HeLa and F9 cells, but not within MPC11 lymphoid cells, indicating a cell-type-specific activity dependent upon necessary cofactors. TEF-1 cDNA was cloned and sequenced three years later by Xiao,⁴³ who used chimeric constructs to show that the C-terminal domain contained a motif that was capable of squelching promoter activity at increasing doses. This suggested that it interacted with a limiting quantity of an unknown cofactor. Farrance et al. subsequently showed that TEF-1 was equivalent to M-CAT binding factor, a regulator of the cardiac troponin-T promoter isolated from chicken muscle.⁴⁴ The GT-IIC and M-CAT sequences are near perfect complements of each other, as can be seen by comparing the reverse complement of the GT-IIC sequence to the M-CAT consensus:



However, the Farrance results also left unanswered whether or not all M-CAT binding factor was identical to TEF-1.

TEF-1 is highly conserved evolutionarily, with strong homology to *Drosophila* scalloped (Sd), a neuronal-specific transcription factor. When Blatt and DePamphilis compared the amino acid sequences for mouse and human TEF-1, they found a striking 99% identity between the two,⁴⁵ with conservation strongest in the amino-terminal portion of the protein. Burglin was first to coin the phrase “TEA Domain” to describe this ubiquitous 66 amino acid DNA binding domain based upon similarity between the human *TEF-1*, yeast *TEC1*, and *Aspergillus* *AbaA* genes.⁴⁶ Hwang et al. subsequently showed that this domain was responsible for the DNA-binding activity of TEF1.⁴⁷

Other members of the TEAD family followed shortly thereafter. By 1996, a total of four paralogs had been identified.⁴¹ TEAD2 (also embryonic TEF) was found by Yasunami et al. in mouse neural precursor cells, and shown to have expression limited strictly to early embryonic neuronal development.⁴⁸ It was subsequently shown to regulate Pax3 expression during neural crest development.⁴⁹ TEAD3 (also TEF-5 or DTEF-1) was found in a screen using a chicken heart cDNA library.⁵⁰ It was expressed primarily in lung and cardiac tissues, with low levels in skeletal muscle. The mouse TEAD3 homolog was cloned shortly thereafter by Yockey et al.,⁵¹ whereas the human homolog was cloned by Jacquemin.⁵² In mammals, TEAD3 has both cardiac and skeletal expression, but highest levels are found within placental tissues where it regulates the chorionic somatomammotropin gene.⁵²

Murine TEAD4 (also RTEF-1) was cloned by Yockey et al. from a Sol8 myotube library.⁴⁰ TEAD4 is most highly expressed in the lung, and like TEAD1, within cardiac and skeletal muscle of the mouse. The human homolog was cloned from a heart cDNA library by Stewart et al.,³⁹ and was found to drive muscle-specific transcription of both the α -myosin heavy chain and skeletal α -actin promoters.⁴² As in the mouse, TEAD4 is expressed in skeletal muscle, with lesser levels in the heart, pancreas, and placenta. However, human TEAD4 is not detectable in lung. TEAD4 is unique from other TEADs in its ability to drive muscle-specific promoter activity during α -adrenergic responses in hypertrophic cardiomyocytes.⁵³

All mammalian TEADs share a gene structure that includes twelve exons, including four in the N-terminal TEA DNA-binding domain, and four in the C-terminal co-factor interaction domain. The TEA/ATTS binding domain consists of a highly-conserved span of 66 amino acids that form three alpha helices. Solution NMR spectroscopy was used to

solve the DNA binding domain structure, confirming earlier suggestions of three helices assembled in a structure resembling a homeodomain fold.⁵⁴ Anbanadam also demonstrated that the specificity of the TEA DNA binding domain is determined largely by the first five nucleotides of the canonical M-CAT sequence, ACATT, with lesser specificity conferred by the 3' nucleotides CCT.⁵⁴

The carboxy-terminal cofactor interaction domain of TEADs bears strong similarity across the entire family. The sequences of multiple TEADs have been shown to interact with both YAP⁶⁵⁵⁵ and TAZ.⁵⁶ In *Drosophila*, the TEAD homolog *Scalloped* is involved in regulation of organ size by Hippo pathway signaling.⁵⁷ Phosphorylation of its co-factor Yorkie (Yki), a YAP homolog, by Hippo causes the cytoplasmic retention of the Sd/Yki complex, preventing transcriptional activation and limiting proliferative responses. Within the human Hippo tumor suppressor pathway, TEAD family proteins were found to be the strongest binders to YAP, suggesting a role in tumorigenesis.⁵⁸ The crystal structure of YAP bound to the carboxy-terminal domain of TEAD1 has been solved, and demonstrates the strong interactions between the two proteins.⁵⁹ ⁶⁰ Subsequent experimentation has shown that disruption of the YAP-TEAD interaction *in vivo* is capable of inhibiting tumor growth in murine liver, confirming the physiological significance of this interaction.⁶¹

TEAD4 REGULATION OF HIF-1 α

Subsequent to the initiation of the present studies, Jin et al. published findings demonstrating that TEAD4 could drive HIF-1 α transcription in BAEC, HMEC, and HUVEC lines.⁶² siRNA knockdown of TEAD4 led to reduced levels HIF-1 α transcription, and its overexpression drove higher levels of HIF-1 α expression. Through the use of chromatin immunoprecipitation, TEAD4 was shown to bind to the HIF-1 α promoter, and a deletion analysis showed that the second of two MCAT-like binding sites was required for TEAD4-

driven activation of promoter activity. Chemical inhibition of HIF-1 α signaling using YC-1 led to a reduction in the ability of TEAD4 to drive EC proliferation and tube formation. In a murine hindlimb ischemia recovery model, the conditional overexpression of TEAD4 led to accelerated healing. These results demonstrated that TEAD4 represents an important upstream driver of HIF-1 α transcription.

REGULATION OF VEGF BY TEAD4 AND HIF-1 α IN MURINE OIR

The finding that TEAD4 regulates HIF-1 α transcription suggested that some of the prior effects of TEAD4 on the VEGF promoter might have been an indirect result of its ability to influence HIF-1 α levels rather than a consequence of TEAD4 binding to the VEGF promoter directly. In this work, we investigated TEAD4 expression within the mouse OIR model, and whether or not TEAD4 regulation of VEGF promoter activity occurs independently of HIF-1 *in vitro*. We show that TEAD4 expression varies from the normal developmental pattern, falling during the vaso-obliterative phase of OIR, and rising during the neovascular phase. Novel TEAD4 isoforms, cloned and sequenced from mouse neural retina, enhanced VEGF promoter activity in hypoxia within gene reporter assays. This enhancement increased under hypoxic conditions, but TEAD4 was found to require HIF-1 α for this effect, indicating that TEAD4-driven increases in VEGF promoter activity are likely due to its ability to modify HIF-1 α expression rather than by direct promoter binding. Finally, we examined the pattern of TEAD4 expression in neovascularized murine retina, finding no detectable expression in Müller glia, but increased expression in endothelial cells of neovascular tufts.

Chapter II. TEAD4 AND VEGF IN AN OXYGEN-INDUCED RETINOPATHY MOUSE MODEL OF NEOVASCULAR DISEASE

A. TEAD4 SPLICE VARIANTS WITHIN WILD-TYPE AND OIR NEURAL RETINA

B. TEAD4 AND VEGF LEVELS IN THE MURINE OIR MODEL

INTRODUCTION

Preliminary studies of the OIR model performed in the Stout lab had demonstrated the presence of *Tead4* mRNA transcripts in lysates of P8 and P17 mouse neural retina.³⁵ However, it was not known if the quantity of TEAD4 varied with disease progression, or if alternate transcripts were present at other timepoints in the OIR model. Studies of RNA from the neural retina of OIR mice from several timepoints were initiated to compare both the quantity and splicing of mRNA transcripts to room-air controls. Timepoints P8, P10, P12, P14, P17, P21, and P24 were chosen to cover the vaso-obliterative, neovascular, and regression phases of OIR, in addition to a wide range of developmental timepoints in room-air controls. RT-PCR was used to investigate alternate splicing of TEAD4, with quantitative real-time PCR and Western blotting showing age-dependent changes in the level of VEGF and TEAD4 that differed from the normal developmental pattern. TEAD4 was found to decrease in parallel with VEGF during the vaso-obliterative phase of the model and increase during the neovascular phase.

RESULTS

TEAD4 SPLICE VARIANTS WITHIN WILD-TYPE AND OIR NEURAL RETINA

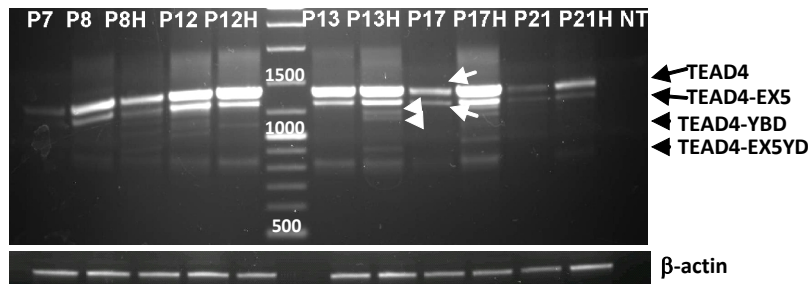
Alternate splice variants of TEAD4 are present in primary human retinal vascular endothelial cells (PRVECs).³⁵ To examine TEAD4 expression patterns within the murine OIR model, RNA was purified from pooled neural retinas dissected from OIR and control mice during the vaso-obliterative, neovascularization, and regression phases of the disease. RT-PCR for TEAD4 using primers located in exons 1 and 12 showed that the dominant transcript was full-length TEAD4 (Figure II.1a). Amplicons for three shorter splice variants were also detected, albeit at lower levels. Sequence analysis revealed that the longest variant (designated TEAD4-EX5) lacked exon 5. Two shorter amplicons (TEAD4-YBD and TEAD4-EX5YD) lacked different combinations of exons 5, 7, 8, and 9 (see Figure II.2). The longer of the two retained exon 5, whereas the shorter lacked this 129bp segment. Interestingly, TEAD4-YBD and -EX5YD shared a frame-shift within the coding region from the splicing of exon 6 to exon 10. This resulted in a novel C-terminus and introduced a premature stop codon within exon 10 that effectively eliminated the majority of the C-terminal, YAP binding domain.

VEGF AND TEAD4 LEVELS IN THE MURINE OIR MODEL

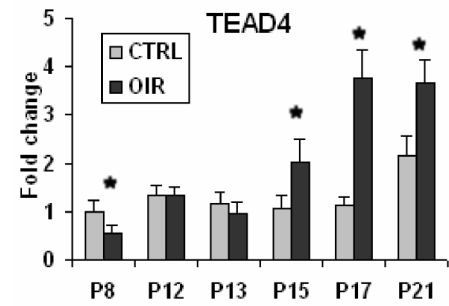
Quantitative RT-PCR for *Tead4* and *Vegf* showed that transcript levels declined within the vaso-obliterative phase of OIR to roughly 50% and 35% of normal P8 developmental levels respectively (Figure II.1b). Upon return to room air conditions (relative hypoxia), *Tead4* and *Vegf* transcript levels increased, with mRNA levels peaking at P17, coincident with maximum neovascularization. Western blots of neural retina protein lysates showed that changes in protein were delayed relative to the changes in transcript levels.

TEAD4 protein had not increased at P12.5, but rose above controls at P13 in protein from treated animals (Figure II.1c). TEAD4 remained above room-air controls at P15, but both began to fall at P17. However, in a pattern similar to transcript levels found by qRT-PCR, TEAD4 protein remained elevated in P17 OIR retinas compared to room-air controls.

A.



B.



C.

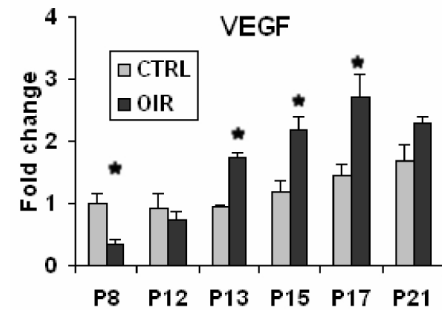


Figure II.1. TEAD4 and VEGF expression patterns over the course of development and OIR progression. (A) RT-PCR showing differences in *Tead4* expression at various timepoints in the OIR model vs. room-air controls. (P=postnatal day, H indicates OIR samples. Lower band, B-actin control.) (B) Real-time, quantitative RT-PCR for *Tead4* and *Vegf* transcripts shows a similar pattern of expression, falling at P8 and peaking at P17. (*= $p < 0.05$, $n = 3$) (C) Western blot for TEAD4 showing elevated levels of protein during the neovascular phase of OIR. (Upper pane, TEAD4; Lower pane, β -actin control.)

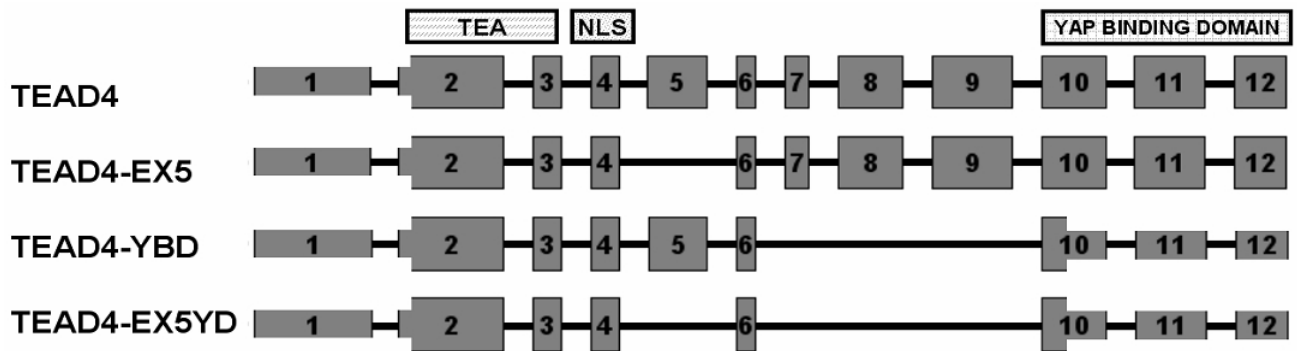


Figure II.2. Four unique TEAD4 transcripts identified within murine retinas: TEAD4, TEAD4-EX5, TEAD4-YBD, and TEAD4-EX5YD. Various combinations of exons 5 and 7-12 were spliced out of the transcripts. The two shorter isoforms lack almost the entire C-terminal co-factor interaction domain. TEA=TEF/TEC/ABAA DNA-binding domain, NLS=Nuclear Localization Signal.

DISCUSSION

In these studies, we found that TEAD4 expression patterns differ within the mouse between normal development and the OIR model at multiple timepoints. Given that TEAD4 is known to bind to and regulate the *VEGF* promoter within multiple EC types, the coincident decreases in *Tead4* and *Vegf* mRNA suggested that TEAD4 might contribute to interruption of the normal developmental vasculogenesis within the OIR retina by reducing *VEGF* transcription. The subsequent coordinated recovery in their levels suggests that TEAD4 might also play a role in increased VEGF production during the neovascular phase, as overexpression of TEAD4 increases VEGF expression within various EC types. There is a lag between increases in *Vegf* and *Tead4* at P13 and P15, which indicates that other transcription factors such as the widely-established HIF-1 pathway are likely involved in the immediate response. Also, the temporal pattern of *Tead4* expression generally matches the degree of retinal neovascularization, suggesting that it may be produced within the tufts themselves.

The pattern observed during the hyperoxic exposure phase of the OIR model suggests a potential intervention whereby measures to sustain TEAD4 might reduce the severity of vaso-obliteration by limiting decreases in VEGF. By extension, it might also be considered as a prospective therapy for infants at risk for retinopathy of prematurity. Alternatively, TEAD4 might be useful as a tool to reduce severity of neovascularization, as exogenous expression of the inhibitory TEAD4₂₁₆ isoform could limit VEGF increases. TEAD4₂₁₆ was shown to inhibit VEGF promoter activity *in vitro*,³⁶ so delivery to the neovascularizing retina could potentially reduce VEGF levels and limit tuft formation.

Alternative splicing of TEAD family transcription factors has been reported by others, with multiple isoforms of TEAD1 having differential ability to regulate the human chorionic

somatomammotropin gene isolated from BeWo human choriocarcinoma cells.⁶³ Within the eye, several isoforms of TEAD4 have been reported from human, non-human primate, and murine neural retina.³⁵ Although there was no clear correlation between disease stage and isoform switching, three isoforms were identified in this work. TEAD4-EX5, lacking exon 5, is identical to a variant found in mouse craniofacial tissues (accession no. NM_201441).⁴¹ The other two, TEAD4-YBD and TEAD4-EX5YD, are similar to isoforms mentioned in an earlier publication by Appukuttan et al.³⁵ Both bear a structure similar to TEAD4₁₄₈ (earlier, RTEF-1₄₄₇) isolated from PRVECs.³⁵ Because these variants lack almost the entire C-terminus, binding to the cofactors YAP or TAZ through this domain is unlikely. However, they retain complete nuclear localization signals. Since YAP and TAZ have been shown to be involved in cytoplasmic retention, it is conceivable that these shorter variants would be preferentially located within the nucleus. As nuclear localization is required for enhancement of gene expression by TEAD family members in other settings, this could increase expression of target genes including *VEGF*. However, the low relative intensity of these bands in semi-quantitative RT-PCR and the lack of verifiable protein data suggest that any physiological role for these variants may be limited.

Overall, the *in vivo* data presented suggest that TEAD4 expression is altered significantly within the OIR model compared to normal development. However, the elevation present during the acutely hypoxic neovascular phase of the disease may be purely correlative in nature. In order to examine the potential for a causal role in increased VEGF transcription within the OIR retina, *in vitro* gene reporter assays were performed using expression plasmids cloned from the TEAD4 variants described above, detailed in subsequent chapters of this work.

MATERIALS AND METHODS

MOUSE MODEL OF RETINOPATHY OF PREMATURITY

C57BL6 mice were bred at the Oregon Health and Science University animal care facility in accordance with National Institutes of Health guidelines and the ARVO Statement for the Use of Animals in Ophthalmic and Vision Research and raised according to the published murine OIR protocol.^{11 64} Briefly, young pups with their nursing mothers were placed in a 75% oxygen environment at postnatal day 7 and returned to room air conditions at postnatal day 12, while control mice were maintained in normal room air. At postnatal days 8, 10, 12, 13, 15, 17, and 21, mice were deeply anesthetized in 100% CO₂ atmosphere and sacrificed. Whole eyes were harvested immediately by cutting the optic nerve, followed by removal of lenses and sclera and dissection of neural retina. Whole RNA was isolated from four pooled retinas using an Ambion RNAqueous kit. Protein was obtained by sonication of four additional pooled retinas in RIPA buffer supplemented with cOmplete mini protease inhibitor cocktail (Roche). For immunohistochemistry, eyes from additional mice were washed in PBS, fixed for 15' in 4% paraformaldehyde, and cryoprotected in progressively increasing concentrations of sucrose solution at 10, 20, and 30% before embedding in OCT freezing compound and cryosectioning at 16um thickness. Sections were maintained at -80C until use.

RT-PCR AND WESTERN BLOTTING

For RT-PCR, 1.0ug of total RNA was reverse transcribed using Omniscript RT Kit (Qiagen) according to manufacturer's instructions. PCR was performed using a primer pair landing in the 5' untranslated region of TEAD4 and exon 12, respectively (5'RTEF and

muRTEFex12R below). Quantitative real-time PCR was performed in quadruplicate to measure levels of TEAD4, VEGF, and GAPDH using SYBR Green. Absolute transcript levels were determined by use of standards, with relative levels determined by subtraction from GAPDH control. TEAD4 primers landed in exon 9 and 10 (mhRTEFex9F, mhRTEFex10R) whereas VEGF primers spanned exons 7 and 8 (VEGFex7aF4, VEGFex8cR1). GAPDH primers used were huGAPDH_FWD & huGAPDH_REV. Significance was determined using Student's t-test (n=4, p<0.05).

Table 1. PCR Primers

FORWARD		REVERSE	
5' RTEF	ACCCTGGGACCGGTCCAACG	MuRTEFex12R	TCCAAGTCTCTCATTCTTTCAC
mhRTEFex9F	GGACATCCGCCAAATCTATGA	mhRTEFex10R	TCTCAACTTTCTCCACCAC
VEGFex7aF4	GATCCGCAGACGTGTAAATG	VEGFex8cR1	CTCCGGACCCAAAGTGCTC
huGAPDH	AGCTGAACGGGAAGCTCACTGG	huGAPDH_REV	GGAGTGGGTGTCGCTGTTGAAGTC

Western blotting was performed by separating 10ug of protein in a 4-20% Tris-Glycine gel and transferring to nitrocellulose membrane for one hour at 60mA. Membranes were blocked in Odyssey blocking buffer (LI-COR Biosciences) for one hour, then incubated overnight with primary antibodies against TEAD4 (Aviva 38276 1:1000, or custom anti-human antibody 1:1000) and β -actin (SIGMA AC-74, 1:50000). Membranes were washed 3X in PBS with 0.1% Tween, incubated with secondary antibody for 45' (LI-COR IRDye 680CW and IRDye 800CW at 1:1000), and washed again in PBS. Western blotting was performed in triplicate. Imaging was performed on an Odyssey scanner (LI-COR Biosciences), with quantitation performed using ImageJ software.

Chapter III. EFFECT OF TEAD4 OVEREXPRESSION ON VEGF PROMOTER ACTIVITY *IN VITRO*

A. HUMAN AND MOUSE VEGF PROMOTER ACTIVATION BY TEAD4
OVEREXPRESSION IN HEK293T CELLS

B. NATIVE VEGF EXPRESSION BY C57M10 AND MIO-M1 UNDER HYPOXIC
CONDITIONS

C. EFFECTS OF TEAD4 OVEREXPRESSION ON VEGF PROMOTER ACTIVITY IN A
MÜLLER GLIAL CELL LINE

INTRODUCTION

Given the increased TEAD4 expression seen in the OIR mouse model and published data showing its ability to regulate the human *VEGF* promoter in hypoxic endothelial cells, a secretable alkaline phosphatase (SEAP) promoter activity assay was established to examine the interaction between the murine forms of TEAD4 and the *VEGF* promoter *in vitro*. First, a series of TEAD4 expression plasmids and VEGF reporter plasmids were constructed to explore the ability of TEAD4 to influence *VEGF* promoter activity. These showed that TEAD4 was capable of increasing *VEGF* promoter activity in HEK293T cells. Next, the mouse and human *VEGF* sequences were compared, revealing differences in a pair of Sp1 sites within the proximal promoter required for TEAD4 activity. However, SEAP reporter assays demonstrated the similar ability of mouse TEAD4 isoforms to enhance activity of both the mouse and human *VEGF* promoter when overexpressed within HEK293T cells, indicating that murine TEAD4 does not require the missing Sp1 binding sites for activity. Cell lines of ocular relevance were then considered for suitability to address the effect of TEAD4 on the mouse *VEGF* promoter. Given that TEAD4 is known to drive *VEGF* promoter activity in various EC types, a pair of endothelial cell lines, HUVEC and RF/6A, was examined for TEAD4 induction under hypoxia. Although prior reports showed that HUVECs responded to hypoxic conditions by upregulation of TEAD4 expression, neither cell line upregulated TEAD4 when exposed to hypoxia in our experiments. As one of the most significant sources of VEGF during the neovascular phase of OIR, Müller glial regulation of this gene is of particular interest. Therefore, a pair of cell lines with Müller glial characteristics (C57M10 and MIO-M1) was examined for *TEAD4* and *VEGF* expression under normoxic, hypoxic, and simulated hypoxic conditions. Although only modest changes in TEAD4 expression occurred, production of *VEGF* transcripts and

protein was particularly pronounced in hypoxic MIO-M1 cells, with secretion increasing greater than ten-fold above normoxic levels. In gene reporter assays within MIO-M1, overexpression of different TEAD4 isoforms increased *VEGF* promoter activity roughly four-fold under normoxic conditions when compared to background, and the effect doubled again under hypoxic conditions. Although the basal increases in *VEGF* promoter activity were maintained when TEAD4 was overexpressed in conjunction with reporters lacking the HRE, *VEGF* promoter activity did not increase further under hypoxia, suggesting the requirement for HIF-1 in the hypoxic induction of activity.

RESULTS

HUMAN AND MOUSE VEGF PROMOTER ACTIVATION BY TEAD4 OVEREXPRESSION IN HEK293T CELLS

Because of the widespread use of the mouse OIR model to investigate neovascular disease, the human and mouse *VEGF* promoters were compared. Analysis using Clustal indicated 67% sequence identity over the proximal 1kb of promoter, but revealed significant differences within the first 100bp upstream of the transcription initiation site, where the human *VEGF* promoter contains four Sp1 sites spanning -95 to -57bp (Figure III.1a). Although the second and third Sp1 sites are conserved within the mouse, the two flanking Sp1 sites are not. Binding of TEAD4 to the Sp1 sites within the human promoter has been shown to increase the *Vegf* promoter activity.³⁴ In particular, human TEAD4 activation of the human *VEGF* promoter requires binding to the first Sp1 site.³⁴ Therefore, we considered the possibility that the absence of the first and fourth Sp1 sites in the mouse *Vegf* promoter would alter the regulation of mouse *Vegf* by TEAD4. Promoter activation assays were used to compare the activity of the mouse and human *VEGF* promoters. The full-length coding regions for all four splice variants of mouse *Tead4* were cloned into pcDNA expression plasmids under the control of the CMV promoter. The *Vegf* proximal promoters from mouse (-1055 to +54 relative to transcription start site) and human (-1082 to +55 relative to transcription start site) were subcloned into promoterless pSEAP reporter plasmids containing a secretable alkaline phosphatase reporter (Figure III.1b). In co-transfected HEK293T cells, overexpression of murine TEAD4 increased activity of the full-length human *VEGF* promoter (huVEGFproF1R3) by six- to eight-fold above no-insert controls under normoxic conditions (Figure III.1c). Co-transfection with the shorter isoforms of *Tead4* (TEAD4-EX5, TEAD4-YBD, and TEAD4-EX5YD) increased activity of

huVEGFproF1R3 to levels comparable to the full length TEAD4 construct. In order to examine whether the missing Sp1 elements would influence promoter activity, reporter assays were repeated using mouse muVEGFproF1R3 constructs. No significant differences were observed between the two. (Figure III.1d)

NATIVE VEGF EXPRESSION BY HUVEC, RF/6A, C57M10, AND MIO-M1 UNDER HYPOXIC CONDITIONS

To further examine the interaction between TEAD4 and the *Vegf* promoter *in vitro*, we next sought a cell line relevant to neovascular disease that exhibited a pronounced transcriptional upregulation of *Vegf* in response to hypoxia. Studies in the literature showing upregulation of TEAD4 in multiple endothelial cell types suggested that an endothelial cell line might recapitulate the *in vivo* effect for *in vitro* investigation. Two EC lines were considered: human umbilical vein ECs (HUVEC) and RF/6A, an EC line of primate ocular origin. Despite published data showing increased TEAD4 expression in hypoxic HUVECs,⁶² examination of protein from these cells did not show any increase (Figure III.2a). Similar experiments using RF/6A also showed no effect of hypoxia on TEAD4 protein levels (Figure III.2b).

Because of the significant role of Müller glia in VEGF production within the OIR model,³³ two cell lines with Müller glial characteristics were also investigated: C57M10 and MIO-M1. The first, a kind gift of Deb Otteson at University of Houston, was isolated from spontaneously immortalized cells of a P10 mouse retina. It expresses a combination of genes typical of mature Müller glia including *Vim*, *Rlbp1*, *Dkk3*, *Clu*, and *Glu1*, with low levels of *Gfap*.⁶⁵ RT-PCR provided evidence of transcripts for both full-length murine TEAD4 and TEAD4-EX5 in total RNA from C57M10 lysates (Figure III.2c). An increase in

expression level between normoxia and hypoxia was explored using quantitative RT-PCR, which indicated no significant upregulation took place (Figure III.2e).

MIO-M1 cells, a kind gift from Astrid Limb,⁶⁶ are a line of human retinal origin that express proteins typical of mature Müller glia, including vimentin, CRALBP, glutamine synthetase, and EGF-R. These expressed transcripts for the human homolog of full-length TEAD4 and TEAD4-EX5 (Figure III.2d). In cells cultured under hypoxic conditions, no increase in TEAD4 or TEAD4-EX5 transcript levels was observed by quantitative RT-PCR.

In order to examine if changes in TEAD4 expression were seen at the protein level, Western blotting of total cellular protein from normoxic and hypoxic MIO-M1 was performed. Although the TEAD4 band migrating at the predicted 52kDa (previously observed in mouse neural retinal lysates) did not increase, a heavier band of around 65kDa had higher intensity (Figure III.2f). Staining with alternative antibodies against TEAD4 also labeled this band, suggesting that it might be a post-translationally modified version of TEAD4. However, this seems to be a species-specific phenomenon only observed in proteins from the human-derived cell line. Herein, TEAD4 proteins from the mouse, including exogenously expressed murine TEAD4, are referred to as TEAD4_{ex}, with the endogenous human isoform labeled TEAD4_{en} for the sake of clarity.

VEGF expression was also examined using qRT-PCR. Although a significant increase was observed in hypoxic C57M10, a much stronger 16-fold increase was observed in MIO-M1 exposed to hypoxia (Figure III.2g). Similarly, VEGF secretion was sharply upregulated in these cells, increasing more than ten-fold from the levels found in cell culture media of cells raised under normoxic conditions (Figure III.2h).

EFFECTS OF TEAD4 OVEREXPRESSION ON VEGF PROMOTER ACTIVITY IN MÜLLER GLIA *IN VITRO*

In order to deliver the expression and reporter plasmids for the SEAP promoter activity assay into Müller glial cell lines, it was first necessary to overcome the challenge of transfecting these cell types. Optimization was performed using the Amaxa nucleofection system according to standard Lonza protocols. Input from the manufacturer led to the use of a handful of transfection programs (X001, X003, X005, and X009), with the finding that X005 yielded the best transfection efficiency without excessive cytotoxicity (Figure III.3).

SEAP assays were then performed in both Müller glial cell lines. TEAD4 overexpression in the C57M10 line did not significantly change the basal activity of the full-length mouse *Vegf* promoter, producing little or no difference in the quantity of secreted alkaline phosphatase compared to no-insert controls (Figure III.4a). However, reporter assays in MIO-M1 exhibited similar results to those within HEK293T cells. All TEAD4 isoforms upregulated the mouse promoter roughly four-fold compared to no-insert controls (Figure III.4b). When the assays were repeated within hypoxic cells, further upregulation was found, with increases exceeding 9- and 16-fold compared to no-insert controls in hypoxia and normoxia, respectively.

Subsequent experiments were carried out to explore the interaction of TEAD4 with the HRE within the *Vegf* promoter in hypoxic MIO-M1. First, a truncated reporter lacking the HRE (muVEGFproF1bR3, -856bp to +55bp relative to the transcription start site) was co-electroporated with the murine *TEAD4* isoforms. The ability of *TEAD4* isoforms to activate the shorter *VEGF* promoter in normoxia was maintained, but additional increases under hypoxia were lost (Figure III.4c). Similarly, a shorter construct missing about 500bp of the VEGF promoter compared to the full length reporter (muVEGFproF2R3, -525bp to +55bp

relative to the transcription start site) retained basal activity above no-insert controls in the presence of TEAD4 isoforms, but its activity also failed to increase under hypoxic conditions (Figure III.4d).

Next, single transfections were performed in order to determine the impact of overexpression of TEAD4 isoforms on endogenous *Vegf* mRNA expression in HEK293T and MIO-M1 cells cultured under hypoxic conditions. No significant differences in the level of VEGF transcripts were detected by qRT-PCR in either cell line (Figure III.5a,c), despite a slight trend of decreased VEGF transcription in MIO-M1 cells. Similarly, overexpression of TEAD4 did not alter levels of secreted VEGF as measured by ELISA when compared to controls in either cell line (Figure III.5b,d).

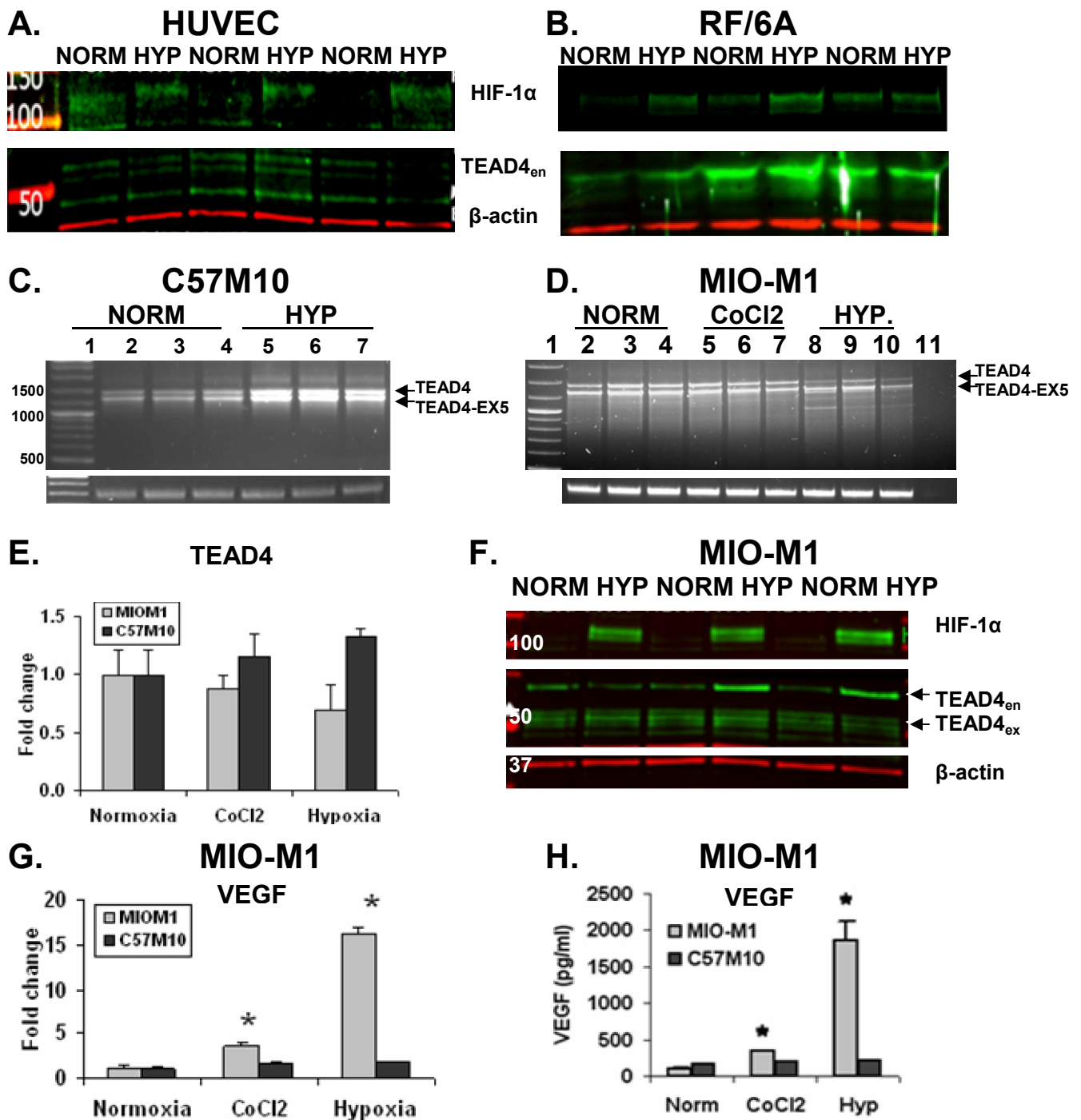


Figure III.2. TEAD4 and VEGF expression *in vitro*. Western blotting showed no change in TEAD4 expression in either (a) HUVEC or (b) RF/6A cells exposed to hypoxia. Top strip=HIF-1 α ; bottom strip: green=TEAD4, red= β actin. (c) RT-PCR in C57M10 showed the presence of TEAD4 and TEAD4-EX5. Lane 1=ladder, 2-4=normoxia, 5-7=hypoxia. (d) RT-PCR in MIO-M1 detected the human TEAD4 and TEAD4-EX5. Lane 1=ladder, 2-4=normoxia, 5-7=CoCl₂, 8-10=hypoxia, 11=no template. (e) Exposure to hypoxic conditions did not produce a significant change in TEAD4 transcription as measured by qRT-PCR in either cell line. (f) No difference was observed in the predicted 52kDa products that labeled with antibodies against TEAD4 on Western blots (TEAD4_{ex}, arrowhead, middle pane) However, a 65kDa band detected by multiple antibodies increased (TEAD4_{en}, arrow). Upper pane, HIF-1 α ; lower pane, β -actin control. Native VEGF expression determined by (g) qRT-PCR and (h) ELISA increased more in MIO-M1 than in C57M10 (* p <0.01, n =3).

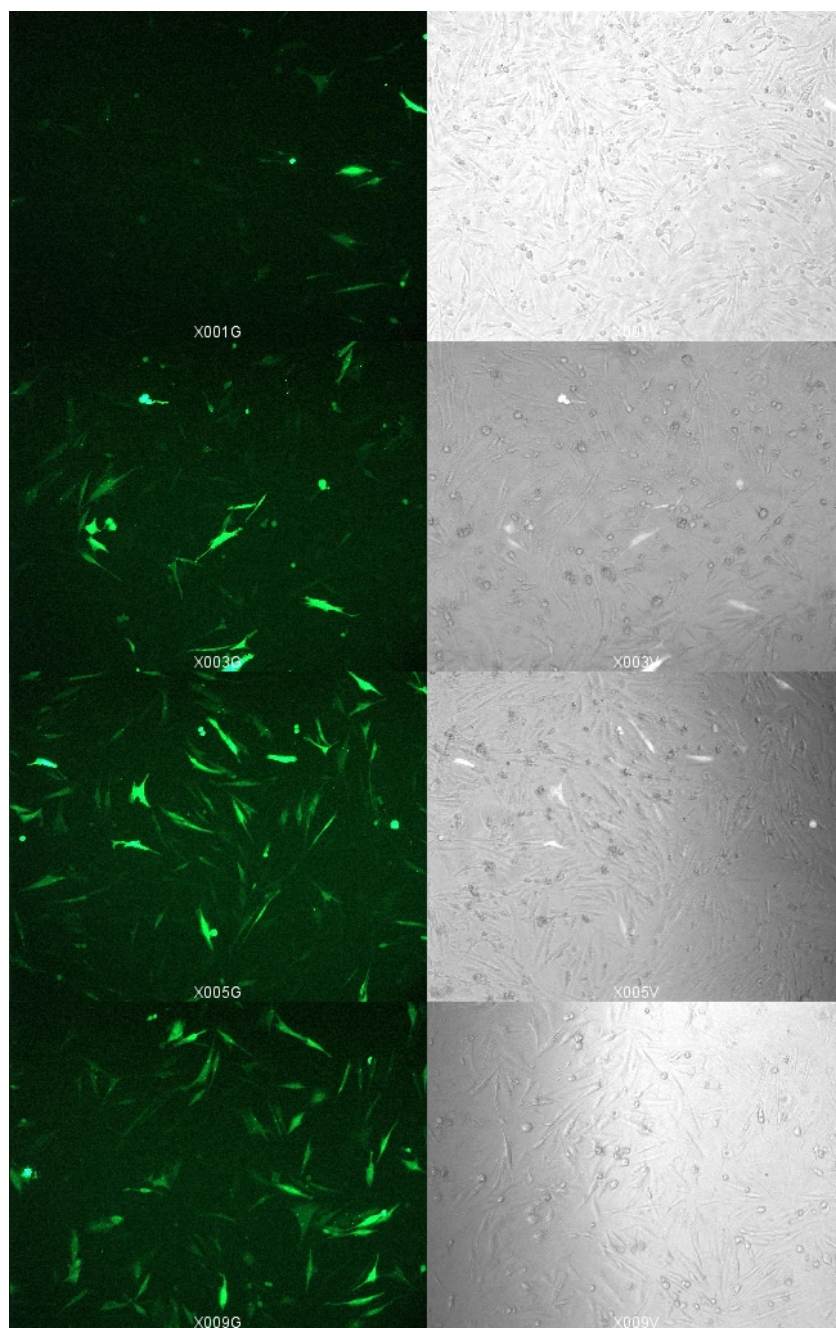


Figure III.3. Fluorescence microscopy images from optimization of Amaxa nucleofection in MIO-M1. Left column, epifluorescence images; right column, phase contrast images. Top to bottom: programs X001, X003, X005, X009. The X005 program yielded the greatest transfection efficiency without causing excessive cell death.

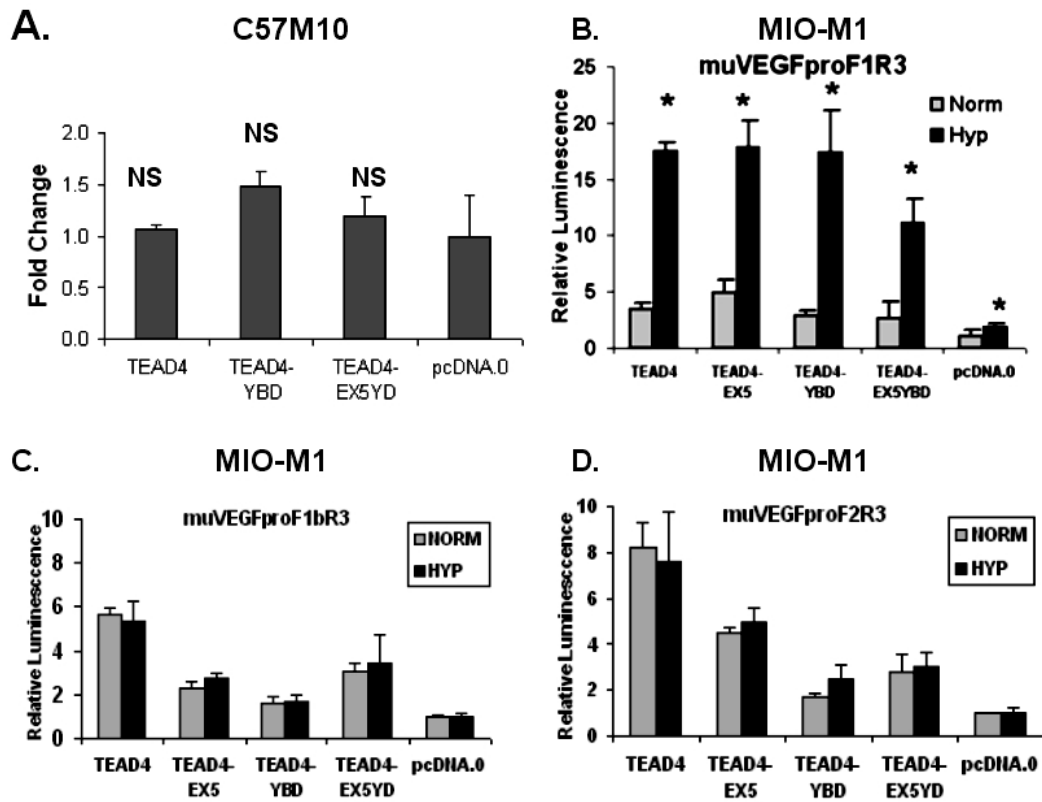


Figure III.4. VEGF promoter activity following TEAD4 overexpression. (A) SEAP reporter assays in C57M10 cells showed no significant change in promoter activation following TEAD4 overexpression when compared to no-insert controls. (NS=not significant, $p < 0.05$, $n = 3$) (B) The same assays in MIO-M1 showed upregulation of the full-length VEGFproF1R3 promoter, which increased further under hypoxia compared to normoxia ($*p < 0.05$, $n = 3$). Hypoxic upregulation was lost in (C) the HRE-deleted VEGFproF1bR3 and (D) the shortest VEGFproF2R3 promoter.

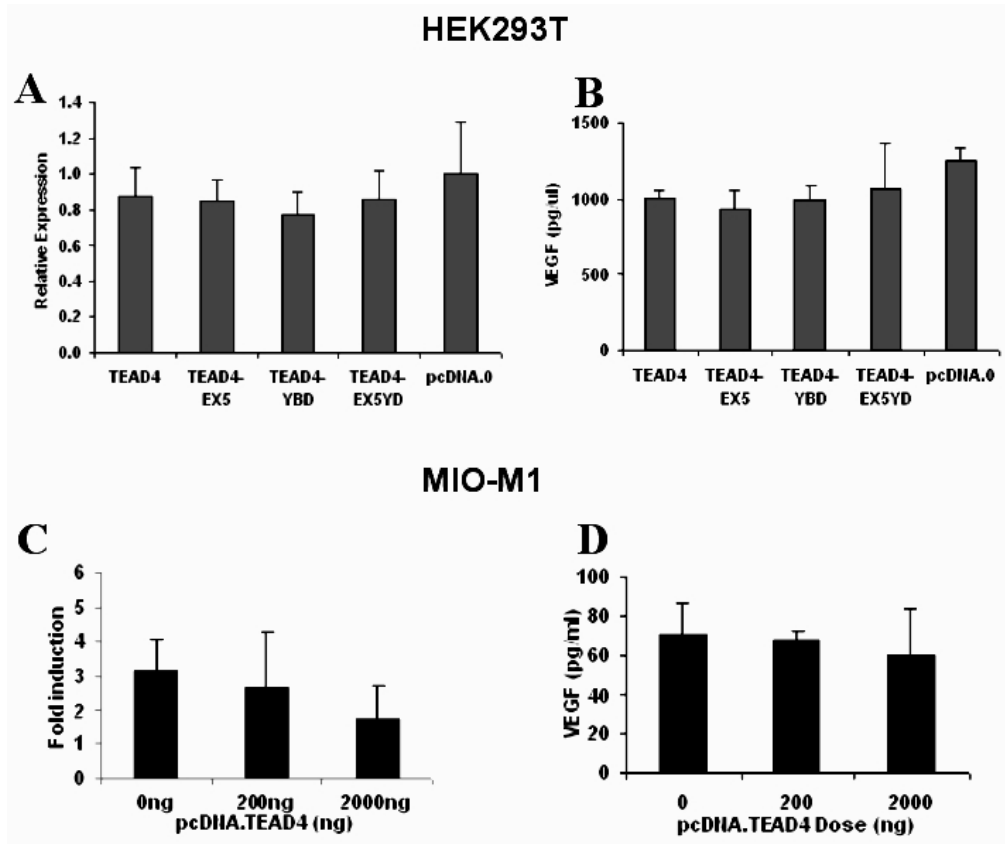


Figure III.5. Effect of TEAD4 overexpression on native VEGF expression levels. (A) Transcription and (B) secretion of VEGF showed no significant changes following overexpression of mouse TEAD4 isoforms in HEK293T. (C-D) Similar results were obtained within MIO-M1 cells for native VEGF (C) transcription and (D) secretion following overexpression of full-length TEAD4 independent of dose.

DISCUSSION

The present studies using murine TEAD4 splice variants from the OIR model overexpressed in HEK293 demonstrated that all four murine isoforms were capable of driving significant increases in *VEGF* promoter activity in a gene reporter assay. These findings are similar to those for the human TEAD4 splice variants published previously.³⁵ Although the mouse exon structures are different than those of the human isoforms, all have in common the presence of the NLS located within exon 4. The presence or absence of the NLS was the most critical factor determining whether a particular human TEAD4 variant acts to enhance or inhibit promoter activity.³⁶ Retention of the NLS was sufficient for activity of enhancer isoforms such as TEAD4₁₄₈, whereas removal of the NLS could eliminate the enhancer activity of human isoforms.³⁶ Although the C-terminal cofactor interaction domain is almost completely missing from TEAD4-YBD and TEAD4-EX5YD, both retain an intact TEA binding domain and NLS. Their ability to drive *VEGF* promoter activity extends this finding to regulation of the murine *Vegf* gene, and suggests that the presence of an intact TEA binding domain and NLS are sufficient structural features to drive *VEGF* promoter activity enhancement in general.

Comparison of the human and murine *VEGF* reporter results shows that there is little difference in the ability of mouse TEAD4 isoforms to activate the promoter from either mammalian species. This is somewhat unexpected, given that the critical Sp1 site shown previously to bind TEAD4 is missing in the murine promoter. However, it is possible that one of the two remaining Sp1 sites in the mouse construct becomes a substitute binding location in the absence of the favored site within the human promoter. Alternatively, murine TEAD4 could bind to a completely different location in the mouse promoter, potentially one of the upstream MCAT-like sequences closer to the HRE.

Although the literature suggested an endothelial cell line as a logical model for *in vitro* examination of the interaction of TEAD4 with the VEGF promoter, neither the HUVEC nor the RF/6A cell lines demonstrated upregulation of TEAD4 in our hands. This was surprising given that published data show upregulation of TEAD4 in HUVECs.⁶² However, there were differences between the applied conditions used for this study and the prior HUVEC work, with 2% FBS used in this study compared to serum-free conditions in the published study. Unfortunately, HUVEC cells cultured under the serum-free conditions used by others failed to survive the 24 hour incubation period of this experiment and required some level of supplementation for survival. Because the conditions could not be replicated identically, it is not possible to determine with certainty whether or not the cells are able to upregulate TEAD4 in response to hypoxia.

The modest upregulation of TEAD4 observed in C57M10 cells suggested that these might be a suitable platform for *in vitro* testing of TEAD4/VEGF promoter interaction. However, these cells had limited induction of VEGF production when exposed to hypoxia, and overexpression of TEAD4 had little effect on *Vegf* promoter activity in this context. In contrast, the effect on *VEGF* transcription of hypoxia in the MIO-M1 line was much stronger, potentially reflecting a species-specific difference between promoter activity between the human and mouse, or perhaps that these cells retain more Müller glial character than the C57M10. The sharp increases in VEGF reflect the integral role that Müller glia play in maintenance of homeostasis within the retina *in vivo*, as demonstrated by earlier studies showing that conditional deletion of VEGF within Müller glia significantly reduced the neovascular response in the OIR model.³³ In that study, both the number of neovascular tufts and the degree of vascular permeability as determined by fluorescein angiography were improved significantly compared to wild-type controls, with

developmental vasculogenesis unchanged. Thus, the much larger hypoxic response by MIO-M1 cells observed in this work seemed to reflect their function *in vivo*. As the larger magnitude of the effect was expected to ease the dissection of the VEGF hypoxic response mechanism, these cells were chosen for all subsequent *in vitro* work.

In *VEGF* promoter activity assays within MIO-M1, TEAD4 overexpression produced upregulation of promoter activity similar to that observed earlier in HEK293 cells. This induction increased further within MIO-M1 exposed to hypoxic conditions, suggesting that TEAD4 might play a role in enhancing VEGF production under hypoxic stress. As it is well established that HIF-1 drives increased *Vegf* transcription under hypoxia, the role of HIF-1 in hypoxic promoter upregulation by TEAD4 was examined using two shorter *Vegf* promoter constructs lacking the HRE. Although TEAD4 isoforms maintained the ability to stimulate activity of both shorter *Vegf* reporters, their ability to enhance promoter activity further under hypoxic conditions was lost, suggesting that TEAD4 requires HIF-1 in order to participate in hypoxic induction of VEGF. As recent studies from the Shie lab have shown, TEAD4 is able to directly modulate HIF-1 expression within human umbilical vein ECs (HUVECs) by binding to the second of two MCAT sequences in the proximal HIF-1 promoter, with overexpression or knockdown of TEAD4 driving increased or decreased levels of HIF-1 transcription and protein, respectively.⁶² The present findings that the HRE is required for hypoxic induction of the *Vegf* promoter suggest that TEAD4 isoforms enhance VEGF promoter activity indirectly within MIO-M1 through their ability to increase HIF-1 levels rather than through direct binding to the *Vegf* promoter (Figure III.4g). In order to determine whether or not a direct TEAD4-VEGF promoter induction occurs in hypoxia, additional experiments involving the manipulation of HIF-1 α levels would be required.

Although promoter activity assays offer interesting insight into transcription factor-promoter interaction, the effect on the native gene is of greater relevance to the understanding of the role of TEAD4 in the OIR model. In this regard, the effects of TEAD4 overexpression within MIO-M1 were limited. Despite indications from enhancement of SEAP reporter transcription, no enhancement of native VEGF expression was found (Figure III.5). Because the promoter activity assays employ supra-physiological levels of transcription factor and reporter, it is possible that more subtle effects present at the much lower physiological levels are hidden. Alternately, elements of VEGF gene structure not captured in the reporter constructs may be at work. As noted by Liu,⁶⁷ there may be multiple elements involved in VEGF regulation, and these may further depend upon the presence of cell-type specific cofactors. In addition to the HRE located upstream of the gene, there is evidence of a 3' enhancer region within the gene.^{68 69} Chromatin structure may also regulate accessibility of TEAD4 to the native gene, another regulatory mechanism not captured in this promoter activity assay.

MATERIALS AND METHODS

VEGF PROMOTER ACTIVITY ASSAYS IN HEK293

SEAP reporter assays using VEGF promoter constructs (see supplemental methods) were carried out in HEK293T cells due to the ease of transfection and the well-characterized nature of this cell line. Cells grown in T75 flasks were split 24-48 hours prior to electroporation and used at roughly 80% confluence. Each TEAD4 pcDNA3.1 expression vector was co-electroporated with mouse or human VEGF promoter pSEAP plasmid in triplicate into 1.0MM cells using the Amaxa nucleofection system, Solution V, and program A-023. A plasmid expressing Metridia luciferase was included to control for transfection efficiency. Electroporated cells were quickly transferred into 12- or 24-well plates containing prewarmed DMEM and maintained for 48 hours in normoxia or hypoxia. Media was collected and analyzed for SEAP using Clontech protocol. Significance was tested using Student's two-tailed t-test with $n=3$, $p<0.05$.

HYPOXIC INDUCTION OF VEGF *IN VITRO*

Two cell lines with Müller glial character, C57M10 (from Deb Otteson, University of Houston) and MIO-M1 (Astrid Limb, Univ. College London), were plated in triplicate into 24-well plates at a density of 100K cells per well. Two endothelial cell lines, HUVEC (Lonza) and RF/6A, were also plated in similar fashion. Plates were maintained in normoxic or hypoxic conditions for 24h. Media was gathered for ELISA, and cells were lysed for RNA by RNAqueous protocol or sonicated in ice-cold RIPA buffer containing cOmplete mini protease inhibitor cocktail (Roche) for protein analysis. cDNA was reverse transcribed from 150ng of total RNA using Omniscript kit (Qiagen) and subject to qRT-PCR in quadruplicate

by previously described protocols for *TEAD4*, *VEGF*, and *GAPDH*. Significance was tested using Student's two-tailed t-test with $n=3$, $p<0.05$.

VEGF PROMOTER ACTIVITY ASSAYS IN C57M10 AND MIO-M1

Transfection into C57M10 and MIO-M1 cells was attempted using both Lipofectamine 2000 and Amaxa nucleofection. For Lipofectamine, C57M10 and MIO-M1 cells were plated overnight at near confluence in 24-well plates in triplicate. Media was removed, and cells were transfected with 1.0 or 2.0ug of pMaxGFP and 1.0, 2.0, or 3.0ul of Lipofectamine 2000 (Invitrogen) in a total of 100ul Optimem. For Amaxa, flasks of cells were trypsinized and electroporated as in the above Amaxa protocol, with the following exceptions. Programs A020, D023, L029, T030, T020, X001, and X009 were used. For MIO-M1, subsequent refinement was carried out comparing programs X013, X009, X005, X003, and X001. Another round of transfections used program X009 and Amaxa solution V or Ingenio electroporation solution (Mirus Bio). Post-electroporation handling was compared using either a rapid transfer into prewarmed plates, delayed transfer (15 minutes), or transfer into 1.5ml Eppendorf tubes before plating.

For SEAP reporter assays in C57M10 and MIO-M1, cells were trypsinized and electroporated in triplicate as in the above Amaxa protocol, except for the use of program X-005. Cells were coelectroporated with 1.0ug of pSEAP reporter plasmid (muVEGFproF1R3, muVEGFproF1bR3, or muVEGFproF2R3), 2.0ug of pcDNA plasmid (TEAD4, TEAD4-EX5, TEAD4-YBD, TEAD4-EX5YD, or no insert control), and 50ng of pMetLuc control. Post-electroporation, cells were gently transferred into 1.5ml Eppendorf tubes and incubated for 30 minutes. Cells were then plated into 12- or 24-well plates containing low calcium RPMI1640 media. After an overnight incubation, media was

changed back to DMEM containing 10% FBS with antibiotic. Plates were maintained in an incubator at 5% CO₂ normoxic conditions, or in a hypoxia chamber flushed twice daily with a 1% O₂, 5%CO₂, 94% N₂ mixture. Media was harvested following 48h of incubation and analyzed for SEAP levels normalized by luciferase controls. Experiments were repeated a minimum of three times, with a representative outcome shown. Significance was established using Student's two-tailed t-test with n=3, p<0.05.

SUPPLEMENTAL METHODS

CONSTRUCTION OF EXPRESSION PLASMIDS AND SECRETABLE ALKALINE PHOSPHATASE REPORTER PLASMIDS

In order to examine the effect of changes in TEAD4 expression levels on VEGF promoter activity, two groups of plasmids were generated. The first included four mammalian expression vectors employing a pcDNA3.1 backbone (Invitrogen); the second included several reporter plasmids generated by subcloning various fragments of the mouse VEGF promoter upstream of a secretable alkaline phosphatase using the Ready to Glow system (Clontech). These are summarized in the table below.

pcDNA3.1 Expression Plasmids

Construction of the TEAD4 expression plasmids began with the RNA isolated from P8, P10, P12, P13, P15, P17, and P21 OIR mice and untreated room-air controls. cDNA was reverse transcribed from 1.0ug of RNA using Omniscript reverse transcriptase (Qiagen) according to manufacturers instructions. TEAD4 was then amplified by PCR from pooled cDNA using a primer pair landing in the 5' untranslated region of TEAD4 and exon 12, respectively (5'RTEF = ACCCTGGGACCGGTCCAACG, muRTEFex12R= TCCAAGTCTCTCATTCTTTTAC). Amplified DNA was separated and visualized using

agarose gel electrophoresis, and four bands were cut for gel purification and reamplification using another round of PCR. Sequencing reactions were then performed on several purified products using BigDye® Terminator v3.1 Cycle Sequencing Kit (Applied Biosystems) with reading performed by OHSU MMI Sequencing Core.

Four unique TEAD4 amplicons were directionally cloned into pcDNA3.1 by restriction enzyme digest (BamHI and XhoI, Fermentas) and subsequent ligation. Ligated products transfected into DH5a E. Coli by 45" heat shock at 42C, and transfectants were selected following overnight incubation on LB ampicillin plates. Colonies were expanded in LB, minipreped, and digested to confirm presence of pcDNA plasmids containing the appropriately sized inserts. Selected clones were then maxipreped in 250mL of LB according to manufacturers instructions (Sigma).

In addition to recovering full-length TEAD4 and a previously-reported variant lacking exon 5, two variants were found with exons 7, 8, and 9 missing. When these sequences were translated *in silico*, it was discovered that a frame shift had taken place in these variants, resulting in a premature stop codon and truncation of the protein product. These two variants were successfully amplified using the linker primers BamKozRTEF_F and muXhoRTEFex10ps. The forward primer appended the *Bam* restriction site and modified the first few base pairs to a valid Kozak consensus sequence, whereas the reverse primer introduced a *Xho* restriction site.

pSEAP Reporter Plasmids

A group of reporter plasmids was constructed by the placement of three segments of the mouse VEGF promoter upstream of a secretable alkaline phosphatase reporter. This was accomplished first through PCR amplification of the appropriate fragment through the use

of several primers listed in the following table. Some of the primers land in regions of sufficient homology such that a single primer could be used with both the human and mouse promoters; primers specific to the mouse are designated with a “mu” prefix.

PRIMER	ANNEALING SITE	SEQUENCE
VEGFproF1	-1055	TGGCCTCAGTTCCTGGCAACATC
VEGFproF1b	-856	CAGTGCCACAAATTTGGTGCCA
VEGFproF2	-580	GTCACTAGGGGGCGCTCGGC
muVEGFproR3	+54	CTcGCCCCCAGtGCCgCGcgCTC

Initial attempts to amplify the mouse VEGF promoter from samples of complete genomic DNA were unsuccessful. Touchdown PCR, gradient PCR, and variations in MgCl₂ were used in an attempt to achieve amplification. Although GAPDH and B-actin positive controls amplified, neither expected product was found. However, PCR to amplify the analogous promoter fragments from human genomic DNA were successful, suggesting that there might be problems specific to the mouse promoter. Off-target binding of primers may have been to blame. The literature contains several reports of difficulty amplifying PCR products from promoter regions of genes related to the high G-C content of promoters. These reports suggested the use of a number of different additives that aided in amplification of GC-rich regions through their putative ability to inhibit secondary structure formation during the annealing phase. PCR additives DMSO, betaine, formamide, and a proprietary secondary structure inhibitor called Q-solution from Qiagen were all used alone and in combination in additional PCRs, but no significant improvement was found. (3/15/10).

An alternate approach was then adopted using a BAC clone RP24-215A3 from the BACPAC Resource Center (Children's Hospital Oakland Research Institute, California, USA) which included the 5' proximal promoter region of mouse VEGF. Bacteria were grown in LB under chloramphenicol selection and miniprepred using manufacturers instructions (Promega). VEGF promoter fragments were successfully amplified using PCR on the less complex template purified from the BAC. Products were gel purified and sequenced, and restriction sites were introduced using primers having an appropriate 5' prefix. VEGF promoter templates and the pSEAP target plasmids were then subject to restriction enzyme digest using NheI and XhoI (Fermentas), gel purified, ligated, and transfected by heat shock into DH5a E. Coli. Successful transfectants were selected by overnight growth on LB plates containing ampicillin, then maxiprepred by manufacturer's instructions (Sigma). Sequences were reconfirmed using ABI Big Dye kit.

Chapter IV. TEAD4 INCREASES VEGF PROMOTER ACTIVITY WITHIN A MÜLLER GLIAL CELL LINE INDIRECTLY THROUGH HIF-1 α

A. EFFECT OF HIF-1 α KNOCKDOWN BY YC-1 ON TEAD4 INDUCTION OF VEGF PROMOTER ACTIVITY

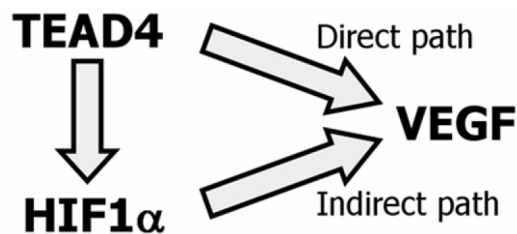
B. VEGF PROMOTER ACTIVITY ON A HIF-1 DEFICIENT BACKGROUND

C. EFFECT OF HIF-1 α AND TEAD4 KNOCKDOWN ON NATIVE VEGF EXPRESSION

D. TEAD4 EXPRESSION IN MÜLLER GLIA AND NEOVASCULAR TUFTS OF MOUSE NEURAL RETINA

INTRODUCTION

Although TEAD4 isoforms were found to induce *Vegf* promoter activity in a SEAP reporter assay in hypoxic MIO-M1 cells, recently published data indicating that TEAD4 is also able to regulate HIF-1 α suggest that these increases might be the indirect result of increased levels of HIF-1 α transcription. This is corroborated by earlier experiments showing that removal of the HRE from the reporter construct eliminated hypoxia-driven increases in VEGF promoter activity. Thus, the focus of this work shifted to examining the contributions of direct regulation of VEGF and indirect contributions secondary to TEAD4-induced changes in HIF-1 α :



Several methods were employed to test the requirement for HIF-1 α , including chemical inhibition, genetic deletion, and RNA interference. First, YC-1 inhibition of HIF-1 α was used to knock HIF-1 α protein levels down to normoxic levels. However, TEAD4 overexpression overcame the YC-1-induced knockdown. Second, a cell line having a point mutation in HIF-1 β was examined for use in the SEAP reporter assay. Despite the complete absence of functional HIF-1, C4 cells exhibited hypoxic induction of VEGF transcription and protein. SEAP reporter assays on this background demonstrated the ability of full-length TEAD4 to significantly upregulate VEGF promoter activity in the absence of HIF-1, but neither wild-type 1C1C7 nor C4 cells showed increased promoter activity in hypoxia. Next, siRNA targeting *HIF-1 α* transcripts was used to reduce HIF-1 α levels. Although hypoxic induction of *Vegf* promoter activity by TEAD4 had been maintained following YC-1 inhibition of HIF-

1 α , it was eliminated by siRNA knockdown of the gene. Finally, siRNA targeting both *TEAD4* and *HIF-1 α* was used in combination to examine the requirement for TEAD4 in hypoxic induction of native *VEGF* in MIO-M1 cells. Knockdown of TEAD4 alone led to reduced *VEGF* transcription, but also reduced *HIF-1 α* transcription. The compound effect of HIF-1 α and TEAD4 siRNA was no different than HIF-1 α alone, precluding the possibility of a direct role for TEAD4 in *VEGF* gene regulation. Finally, we returned to the OIR model in order to determine the cell populations responsible for TEAD4 upregulation *in vivo* by double-labeling immunohistochemistry. Although no expression was observed within Müller glia, labeling was robust within ECs of neovascular tufts.

RESULTS

EFFECT OF HIF-1 α KNOCKDOWN BY YC-1 ON TEAD4 INDUCTION OF VEGF PROMOTER ACTIVITY

Although TEAD4 isoforms activated the *Vegf* promoter in SEAP reporter assays within MIO-M1 cells cultured under hypoxic conditions, it is possible that the TEAD4-driven increases observed in Figure III.4 were the indirect result of increased levels of *HIF-1 α* transcription. To determine if HIF-1 α was required for TEAD4 activation of the *VEGF* promoter, we repeated promoter activation assays in conjunction with multiple strategies to knock down HIF-1 α . HIF-1 α can be inhibited by YC-1, a small molecule activator of soluble guanylyl cyclase that causes a reduction in HIF-1 α protein levels.⁷⁰ In hypoxic MIO-M1 cells, YC-1 reduced HIF-1 α protein levels in a dose-dependent manner, as measured by Western blotting densitometry (Figure IV.1a). At 50uM YC-1, HIF-1 α was reduced to near normoxic levels. However, at 100uM, YC-1 exhibited cytotoxicity.

When the prior SEAP reporter assays were repeated in MIO-M1 cells with and without YC-1 inhibition of HIF-1 α , full-length TEAD4 drove a five-fold increase in activity of the longest VEGF promoter μ VEGFproF1R3. This effect was not changed significantly in the presence of YC-1 (Figure IV.1b). However, subsequent Western blotting for HIF-1 α showed that the overexpression of TEAD4 sustained HIF-1 α levels, reversing much of the effect of YC-1 treatment (Figure IV.1c). In order to prevent masking of the effect of YC-1, the experiment was repeated with a reduced dose of TEAD4. In MIO-M1 cells, both with and without YC-1 inhibition of HIF-1 α , overexpression of full-length TEAD4 drove a similar 1.5-fold increase in *Vegf* promoter activity in hypoxia compared to normoxia (Figure IV.1d).

Earlier experiments showed that overexpression of TEAD4 produced little impact on native *VEGF* transcription despite increases seen in many promoter assays. In order to test

if the effect of TEAD4 on native VEGF was being masked by the presence of HIF-1 α , these experiments were repeated in YC-1 treated cells. Despite the reduced level of HIF-1 α due to the inhibitor, no significant effect of TEAD4 overexpression on native *VEGF* transcription was observed at either TEAD4 dose tested (Figure IV.1f)

VEGF PROMOTER ACTIVITY ON A HIF-1 DEFICIENT BACKGROUND

Although YC-1 treatment or transfection of siRNA significantly reduces levels of HIF-1 α , neither approach eliminates protein expression completely. In order to exclude the potential for residual levels of HIF-1 α to influence promoter activity, a cell line with a mutation that prevents expression of the complete HIF-1 heterodimer was chosen for use in SEAP promoter activity assays. C4 cells have a mutation that results in a severely truncated form of HIF-1 β (ARNT), preventing it from binding HIF-1 α . First, C4 cells and the 1C1C7 wild-type parental line were examined for expression of native *Vegf* and *Tead4*. By RT-PCR, it was shown that both cell types expressed *Vegf* as well as the two longer *Tead4* isoforms, the full-length and TEAD4-EX5 (Figure IV.2a). Evidence for TEAD4 protein was also present in Western blots (Figure IV.2b).

In order to determine if C4 cells responded to hypoxia with upregulation of *Vegf*, *Vegf* transcription was analyzed by qRT-PCR. Although *Vegf* upregulation was not as pronounced as the four-fold increase delivered by wild-type 1C1C7 cells, C4 cells lacking functional HIF-1 still exhibited a 60% increase in VEGF transcription (Figure IV.2c).

SEAP gene reporter assays were then repeated within the HIF-1-deficient cell line to determine if the absence of HIF-1 impacted the effect of TEAD4 on *Vegf* promoter activity. The results show the almost complete loss of enhancement of *Vegf* promoter activity by most TEAD4 isoforms in both wild-type and HIF-1 β -deficient cells. There was a slight but

significant increase in *Vegf* promoter activity following overexpression of full-length TEAD4 in wild-type cells that did not appear in the C4 line. However, TEAD4-YBD drove a two-fold increase in promoter activity under both normoxic and hypoxic conditions in both cell lines (Figure IV.2d,e). No hypoxic induction was observed in either cell line with any of the TEAD4 isoforms.

EFFECT OF HIF-1 α AND TEAD4 KNOCKDOWN ON VEGF EXPRESSION

Next, we tested if TEAD4 induction of *Vegf* promoter activity was dependent on HIF-1 α by using a pair of siRNA constructs against human HIF-1 α . Both constructs exhibited better than 75% reduction in levels of HIF-1 α transcripts and protein (Figure IV.3a,b). In SEAP assays that included siRNA knockdown of HIF-1 α , TEAD4-driven activity of the *Vegf* promoter in normoxia was roughly five-fold above background, unchanged from cells treated with scrambled controls. However, the hypoxia-dependent increase in *Vegf* promoter activity by TEAD4 was no longer detected in cells co-transfected with the HIF-1 α siRNA (Figure IV.3c,d).

Although TEAD4 overexpression did not increase transcription of the endogenous *VEGF* gene in MIO-M1 cells, we hypothesized that TEAD4 might be necessary for induction of *VEGF* transcription in hypoxia. Therefore, *TEAD4* knockdown was performed using published siRNA sequences⁶² (Figure IV.4a,b). The treatment reduced *VEGF* transcription significantly after four days, but analysis of *HIF-1 α* expression revealed a similar pattern to *VEGF*, indicating that the effect might be secondary to reductions in HIF-1 α (Figure IV.4).

In order to determine if a HIF-1 α -independent pathway for TEAD4 up-regulation of native *VEGF* transcription in hypoxia existed in MIO-M1, cells were treated with siRNA

targeting both HIF-1 α and TEAD4 and exposed to hypoxic conditions. Although HIF-1 α knockdown alone reduced overall *VEGF* transcript levels as determined by quantitative RT-PCR, it did not completely abolish the hypoxia-inducible increase in *VEGF* transcription (Figure IV.5). However, the compound effect of TEAD4 and HIF-1 α knockdown produced little change in *VEGF* transcription compared to HIF-1 α alone.

TEAD4 EXPRESSION IN MÜLLER GLIA AND NEOVASCULAR TUFTS OF MOUSE NEURAL RETINA

In order to examine the cellular localization of TEAD4 expression within the retina, cryosections cut from P17 neural retina at the peak of neovascularization were analyzed by double-labeling immunohistochemistry for TEAD4 and GLAST, a marker of Müller glia. Within nuclei of GLAST-positive cells located in the inner nuclear layer having morphology and location consistent with that of Müller glia, no TEAD4 labeling was observed (Figure IV.6a). Other INL nuclei expressed higher levels of TEAD4, including larger instances that, based upon morphology and position, may represent amacrine cells.

In sections from P17 OIR animals, TEAD4 immunostaining showed a similar pattern of expression, with an absence of staining in GLAST-labeled cells of the INL (Figure IV.6b). However, the most striking difference compared to normoxic controls was the presence of robust staining for TEAD4 in the neovascular tufts of P17 OIR mice. Double-labeling with *Griffonia simplicifolia* isolectin identified these as endothelial, with TEAD4 staining restricted to neovascular tufts and a subpopulation of ECs within deeper established vessels (Figure IV.6e-f).

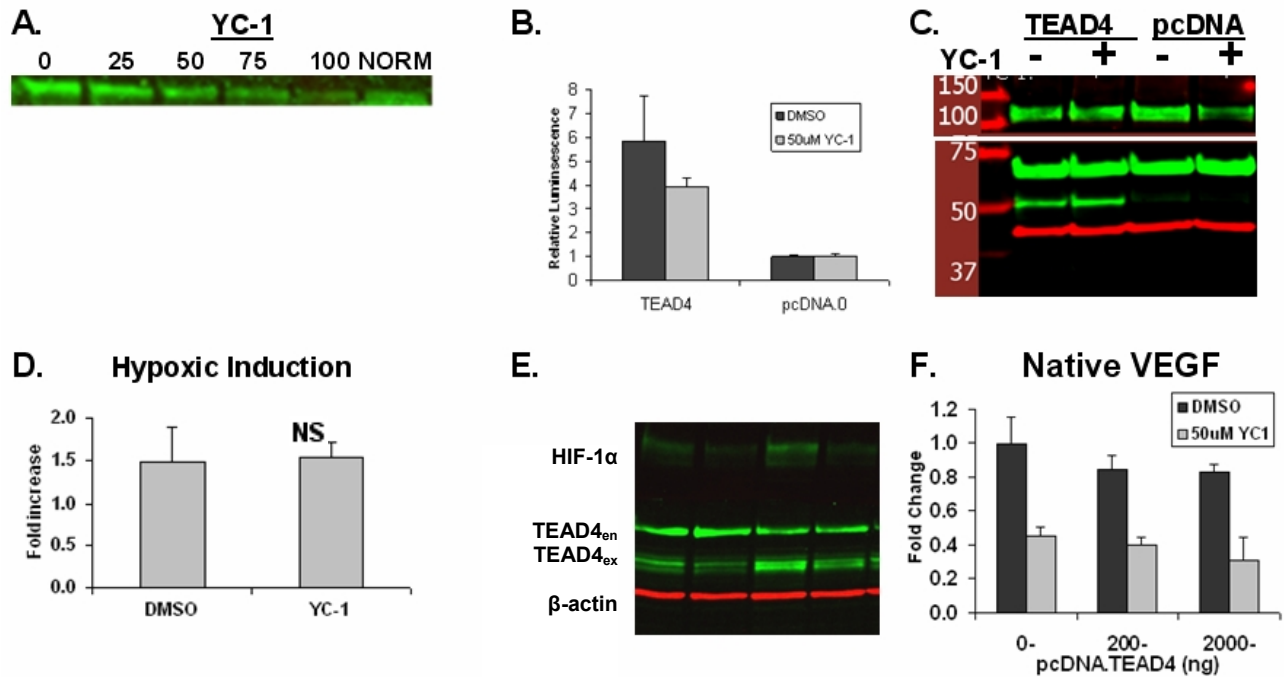


Figure IV.1. Effect of HIF-1 α inhibition by YC-1 on VEGF promoter activity in hypoxic MIO-M1 cells (A) YC-1 Inhibition of HIF-1 α resulted in a reduction of protein expression to near normoxic levels at 50 μ M dose. (green =HIF-1 α , red= β -actin) **(B)** YC-1 inhibition did not significantly reduce induction of VEGF promoter activity in hypoxia by SEAP assay following TEAD4 overexpression ($p < 0.05$, $n = 3$), but **(C)** TEAD4 sustained HIF-1 α expression as shown by Western blot. (top pane, green =HIF-1 α . Bottom pane, green=TEAD4, red= β -actin) **(D)** YC-1 inhibition of HIF-1 α did not reduce induction of VEGF promoter activity in hypoxia compared to vehicle as measured by qRT-PCR following reduced-dose TEAD4 overexpression ($p < 0.05$, $n = 3$). **(E)** Western blot for HIF-1 α and TEAD4 following YC-1 inhibition **(F)** TEAD4 overexpression did not lead to upregulation of native VEGF transcription as shown by qPCR for VEGF even in the presence of HIF-1 α knockdown by YC-1. ($p < 0.05$, $n = 3$)

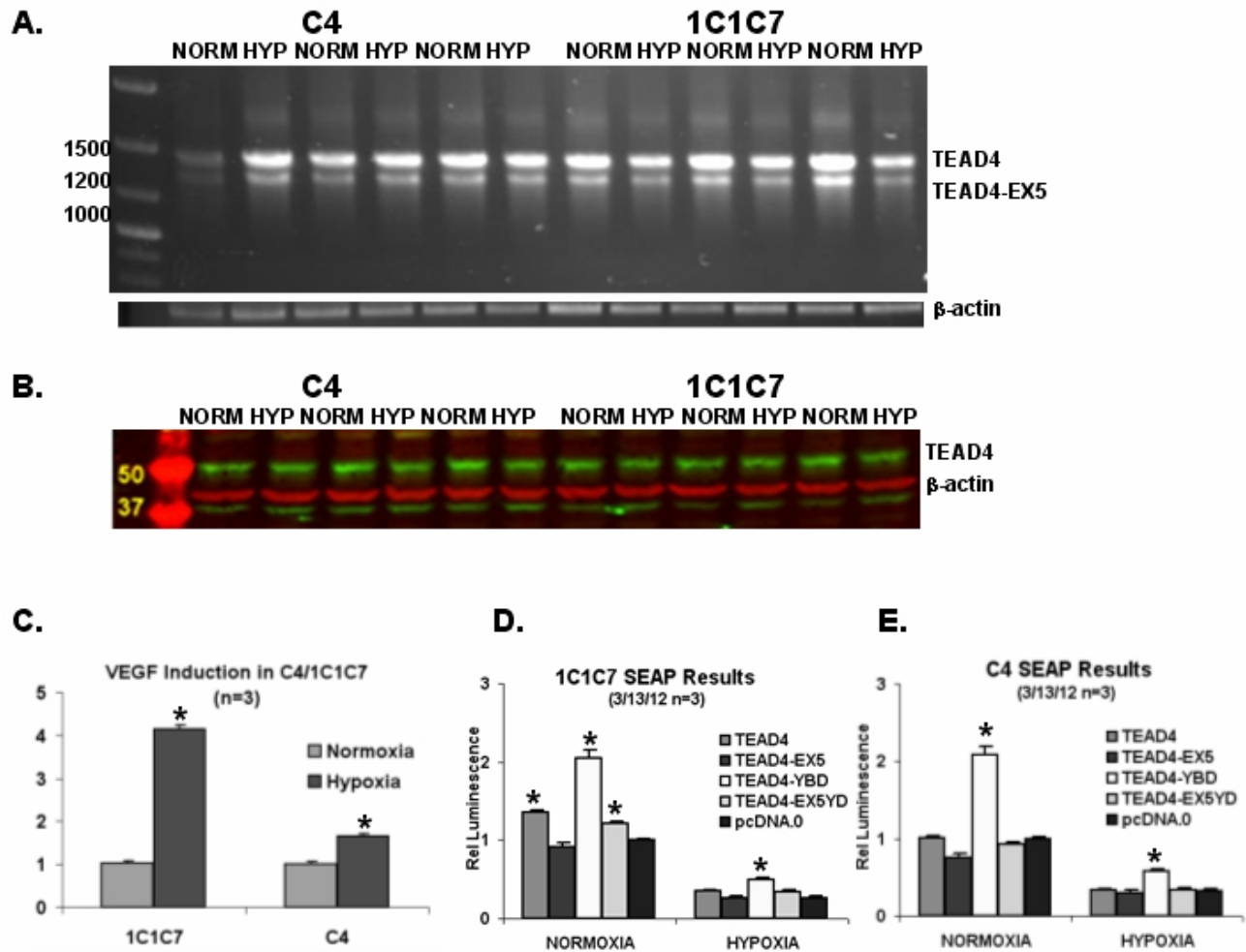


Figure IV.2. *Vegf* promoter activity in a HIF-1-deficient cell line. (A) Wild-type 1C1C7 and HIF-1-deficient C4 express TEAD4 and TEAD4-EX5. (Bottom row, β -actin control) (B) TEAD4 protein expression (green) did not vary between normoxia and hypoxia in either cell line. (green=TEAD4, red= β -actin) (C) Both 1C1C7 and C4 cells exhibit increased production of *Vegf* transcription in hypoxia. (D-E) SEAP reporter assays in C4 and 1C1C7 cells showed no hypoxic induction effect following overexpression of any of the murine TEAD4 splice variants. Only TEAD4-YBD retained the ability to enhance VEGF promoter activity in C4 cells. (* $p < 0.05$, $n=3$)

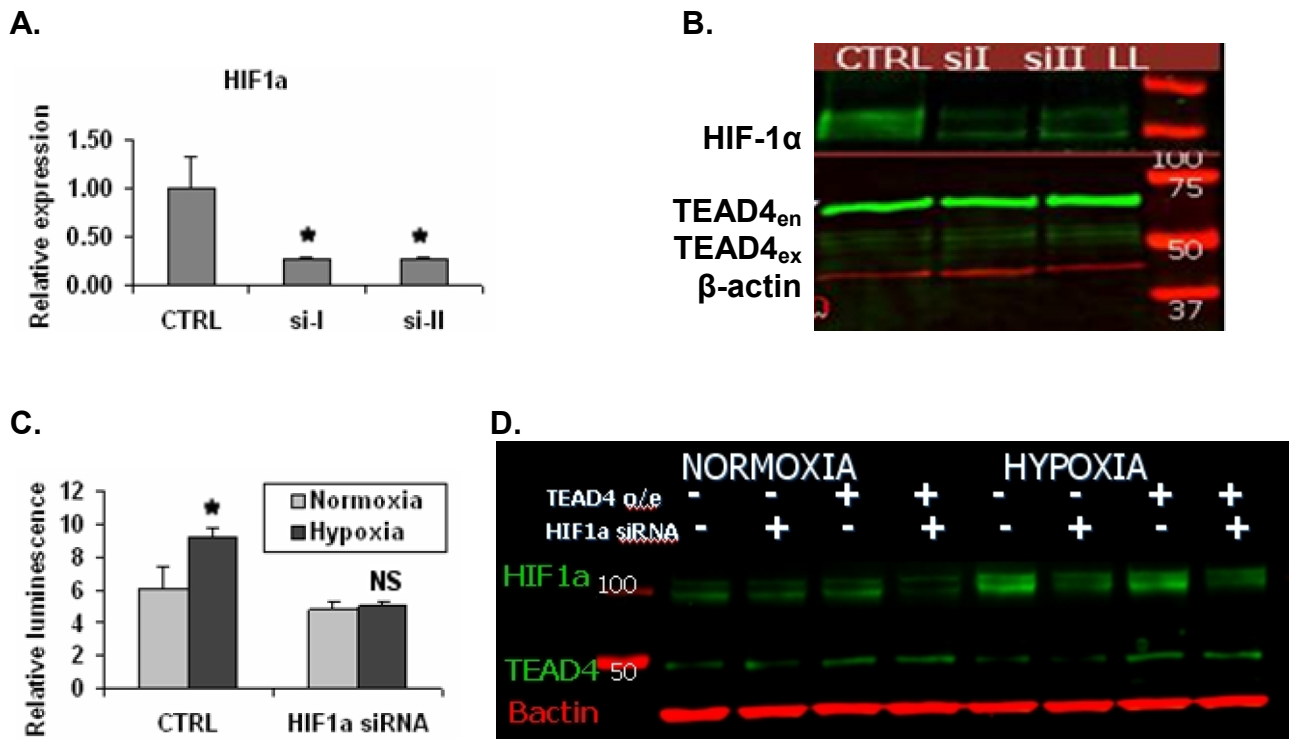


Figure IV.3. siRNA knockdown of HIF-1 α in MIO-M1 cells. Electroporation of siRNA targeting HIF-1 α was successful in knocking down the level of (A) transcripts and (B) protein (C-D) RNA inhibition of HIF-1 α eliminated hypoxic induction of *VEGF* promoter activity when compared to normoxic controls (* $p < 0.05$, $n = 3$, NS=not significant). (D) Western blot showing HIF-1 α and TEAD4_{ex} expression (green). Red= β -actin.

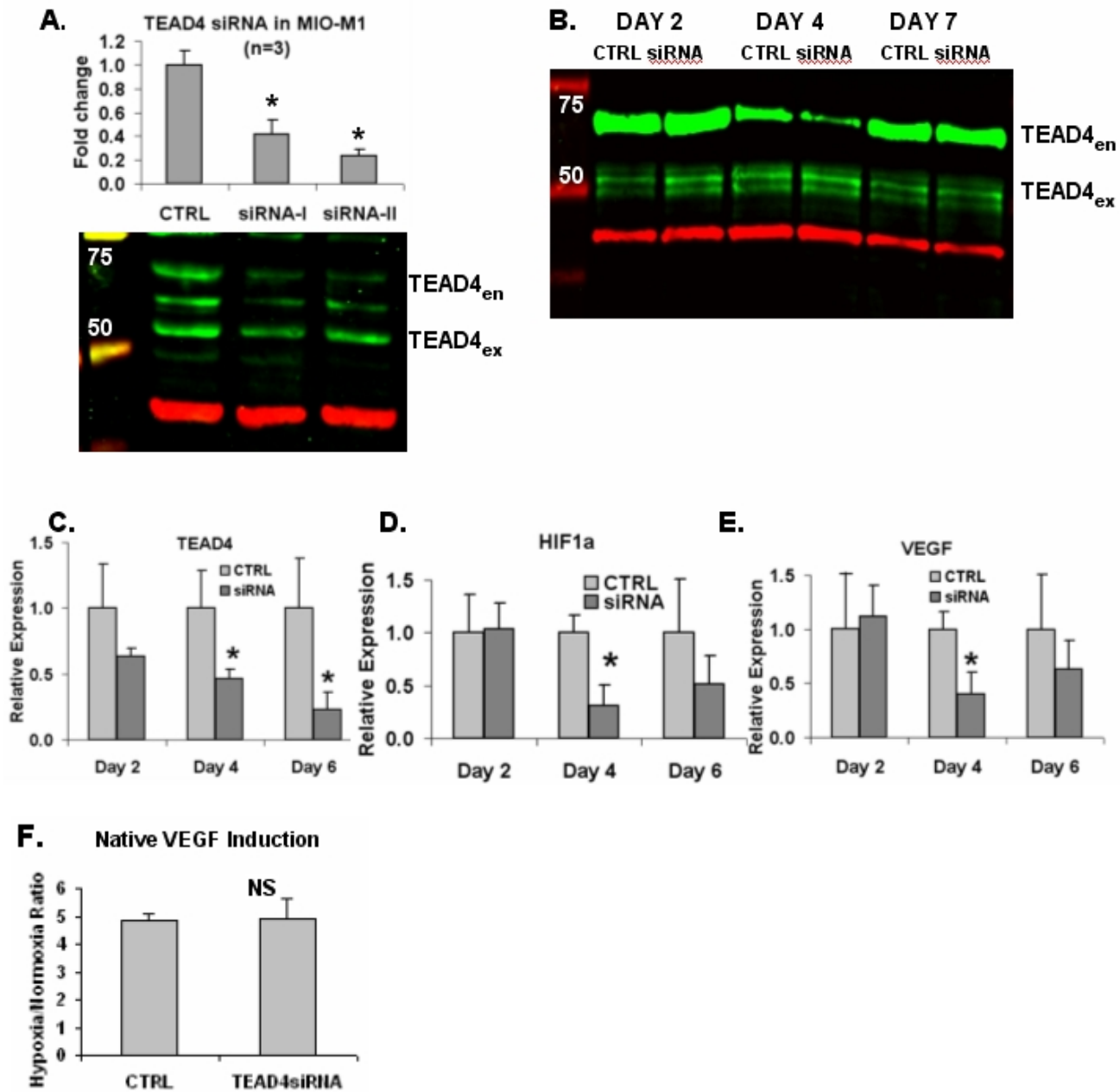


Figure IV.4. siRNA knockdown of TEAD4 in MIO-M1 cells. (A) Electroporation of siRNA targeting TEAD4 reduced transcript levels by up to 80% after 96 hours ($p < 0.05$, $n = 3$), with reductions evident in the 65kDa TEAD4_{en} protein using a custom antibody. (B) In a separate time course experiment, labeling with the Aviva antibody showed that 65kDa TEAD4_{en} protein fell on day 4. (C-E) VEGF levels fell significantly on day 4, coincident with decreases in (C) TEAD4 and (D) HIF-1 α expression. (* $p < 0.05$, $n = 3$) (F) MIO-M1 exhibited similar increases in native VEGF transcription under hypoxia when compared to normoxia with or without knockdown of TEAD4.

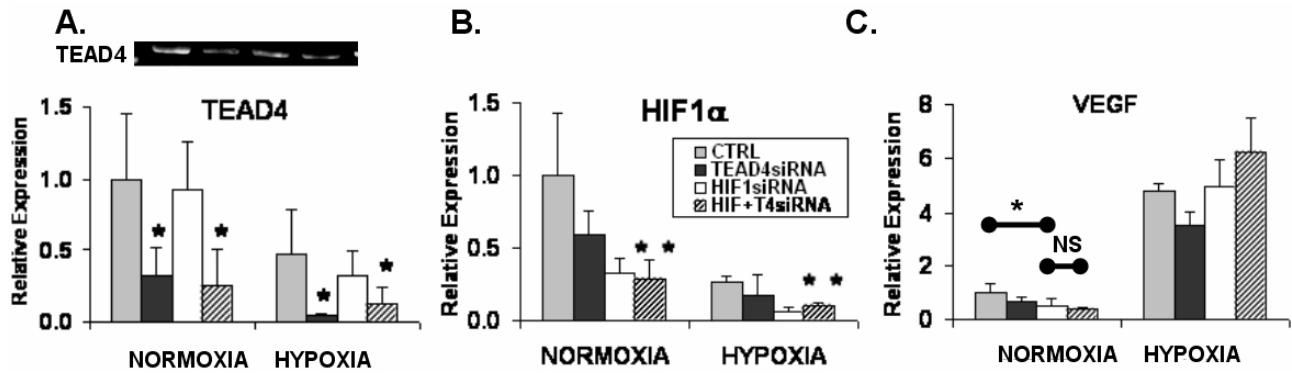


Figure IV.5. Quantitative RT-PCR in MIO-M1 cells treated with TEAD4 and HIF-1 α siRNA. (A) TEAD4 qRT-PCR. TEAD4 siRNA reduced TEAD4 transcription significantly. (B) HIF-1 α qRT-PCR. Reductions in HIF-1 α transcription following TEAD4 siRNA did not reach statistical significance. (C) VEGF qRT-PCR. Although knockdown of HIF-1 α alone led to significant reductions in VEGF transcription under normal oxygen conditions, the effect of TEAD4 knockdown alone was not significant. (*=p<0.05, NS=not significant, n=3) The compound effect of TEAD4 and HIF-1 α knockdown did not have a significant impact on VEGF transcription when compared to HIF-1 α siRNA alone. Under hypoxic conditions, no significant change in VEGF transcription was observed with either siRNA treatment.

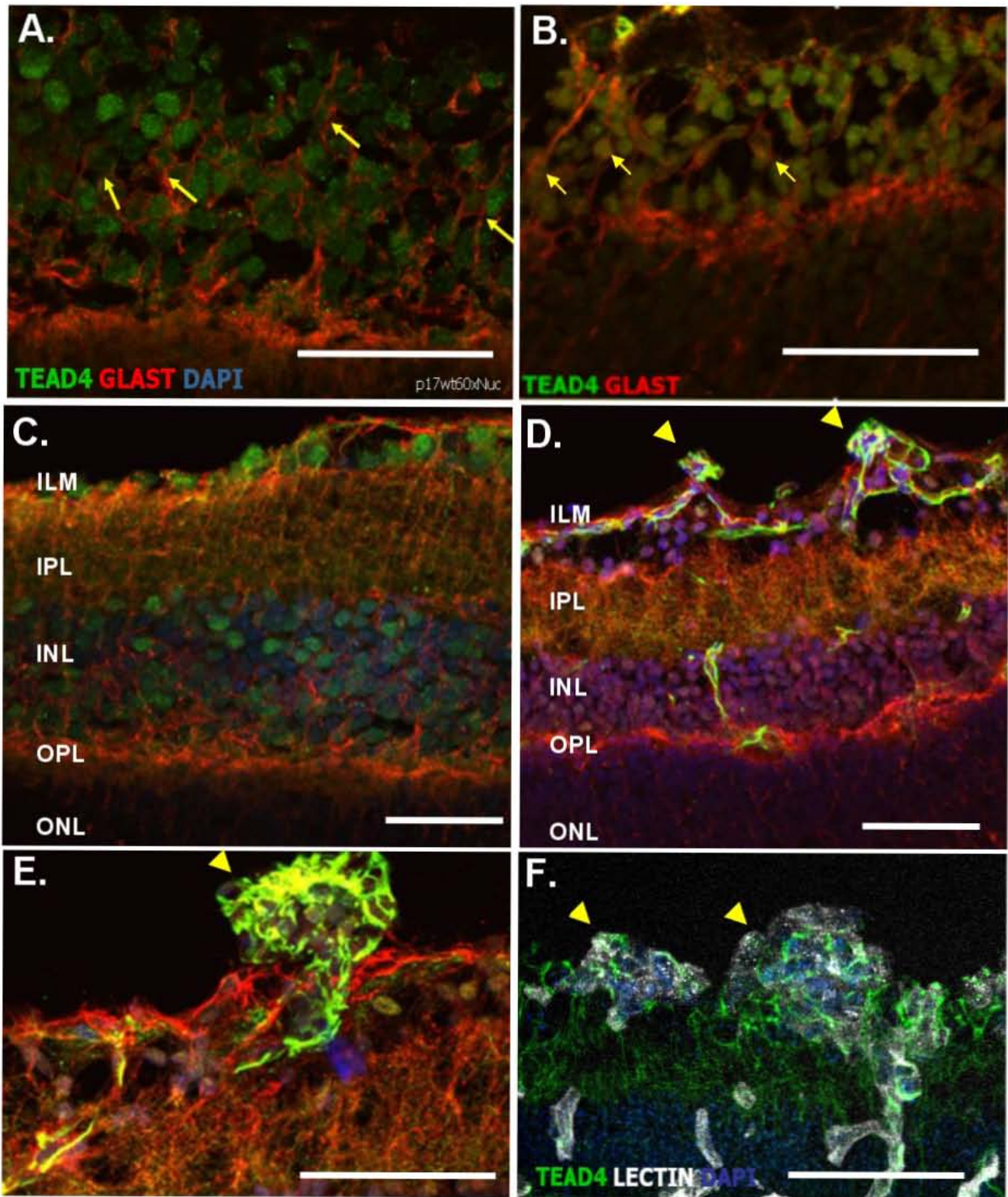


Figure IV.6. . TEAD4 and GLAST immunostaining of P17 mouse neural retina. INL of retinas from (A) WT and (B) OIR mice showing minimal expression of TEAD4 in cells having a Müller glial staining pattern and morphology. (C-D) Broader section of retina comparing (C) WT and (D) OIR sections. Exposure was adjusted to prevent saturation of the signal. (ILM=inner limiting membrane, IPL=inner plexiform layer, OPL=outer plexiform layer, ONL=outer nuclear layer) (E&F) Neovascular tufts stained strongly for TEAD4 (arrows, Müller glia; arrowheads, NV tufts; scale bars = 50 μm).

DISCUSSION

Initial VEGF promoter activity assays performed following chemical inhibition of HIF-1 by YC-1 showed little change in hypoxic induction of VEGF promoter activity, suggesting that TEAD4 might play a HIF-1-independent role in VEGF transcription (Figure IV.1). However, it was found that HIF-1 α levels were restored by TEAD4 overexpression. These results confirm the potential for TEAD4 to regulate HIF-1 α expression in an ocular-relevant cell line, similar to results of Yi Jin within BAECs, HUVECs, and HMECs.⁶² However, this limited our ability to draw conclusions regarding direct TEAD4 regulation of VEGF using this approach.

By using cells harboring a point mutation in ARNT, it was possible to examine the influence of TEAD4 isoforms on the *Vegf* promoter in the complete absence of functional HIF-1. Interestingly, C4 cells maintained a significant hypoxic response in *Vegf* transcription despite the mutation (Figure IV.2). While the majority of the response was eliminated, the remaining increase is likely the result of a HIF-1-independent mechanism. SEAP reporter assays carried out in wild-type cells demonstrated a small but significant effect of full-length TEAD4 and the shortest isoform TEAD4-EX5YD on the *Vegf* promoter. The loss of this effect in C4 cells indicates that they most likely act indirectly through HIF-1 α to drive increased *Vegf* promoter activity in 1C1C7 cells. However, the TEAD4 isoform lacking the YAP-binding domain was able to drive enhanced promoter activity in either cell line, showing an isoform-specific ability to drive *Vegf* promoter activity in a HIF-independent manner. The nature of this isoform-specific behavior would be an interesting avenue for future inquiry. Unfortunately, the lack of hypoxic induction of promoter activity within these cells prevented further dissection of the direct and indirect contributions of TEAD4 to VEGF upregulation in hypoxia.

As the final approach to test HIF-1 α independence, SEAP assays performed in MIO-M1 cells treated with HIF-1 α siRNA exhibited only a slight reduction in *VEGF* promoter activity compared to scrambled controls. This demonstrated that TEAD4 is able to support *VEGF* promoter activity under normoxic conditions despite the loss of HIF-1 α . Whereas the basal level of TEAD4 enhancement was maintained within normoxic MIO-M1, its ability to stimulate promoter activity further under hypoxic conditions was lost. These data support the results of earlier experiments involving *Vegf* promoter constructs lacking the hypoxia response element, providing additional evidence that hypoxic induction of *VEGF* by TEAD4 overexpression is largely an indirect result of its stimulation of HIF-1 α transcription.

A final strategy to assess any independent role of TEAD4 in native *VEGF* induction under hypoxia was to vary the level of TEAD4 expression in the presence of RNA interference for HIF-1 α . These studies demonstrated that reductions in TEAD4 could independently reduce HIF-1 α transcription, extending the earlier findings of Jin *et al.*⁶² beyond the context of endothelial cells. However, when both TEAD4 and HIF-1 α were knocked down in a compound siRNA experiment (Figure IV.5), the lack of any significant additional effect following knockdown of TEAD4 confirms that it is unable to independently drive native *VEGF* transcription within MIO-M1 cells. Interestingly, the increases in native *VEGF* transcription in hypoxia were maintained following compound HIF-1 α and TEAD4 knockdown, again suggesting that a HIF-1-independent pathway for VEGF upregulation does exist, although it does not seem to involve TEAD4.

Müller glia have been shown to be a leading source of VEGF production during the neovascularization phase of OIR, and selective ablation of VEGF within Müller glia can reduce neovascularization in the mouse OIR³³ and streptozotocin-induced diabetic retinopathy models.⁷¹ Therefore, we wished to examine their role in the production of

TEAD4 observed within retinal homogenates. TEAD4 was not found within Müller glial instances of the inner nuclear layer of P17 OIR mice, and it did not appear to vary from normal development (Figure IV.6). Expression appeared to be restricted to Müller glial processes of the IPL and OPL. Although its location outside the nucleus would prevent it from directly participating in DNA binding, the functional significance of cytoplasmic retention of TEAD-family proteins has been noted by others. In the *Drosophila* Hippo signaling pathway, phosphorylation of co-factor Yorkie (Yki) on S168 causes binding by 14-3-3, which prevents nuclear importation of cofactor Scalloped (Sd), a TEAD4 homolog.⁵⁷ Yki is a homolog of the mammalian YAP oncogene, a cofactor that binds to the C-terminal domain of TEAD-family proteins. Phosphorylation at S111 or S250 also led to cytoplasmic retention of the Sd/Yki complex in a 14-3-3-independent fashion. Similarly, the inhibitory TEAD4₂₁₆ isoform has been shown to have cytoplasmic localization within mammalian cells due to the absence of a nuclear localization signal. However, it is able to competitively inhibit activator TEAD4 isoforms despite this location,⁷² so there is evidence for the ability of TEAD4 isoforms to influence transcription even in the absence of nuclear importation.

Given the high levels of expression observed within neovascular tufts of sections from OIR retinas, the increases in TEAD4 within retinal homogenates were more likely due to expression by endothelial cells than by Müller glia. Although this suggests that manipulation of TEAD4 within Müller glia of the neovascularizing retina is not likely to be a productive therapeutic strategy, TEAD4 expression by endothelial cells within neovascular tufts represents a distinctive target for the pathological hallmark of neovascular disease. Whereas HIF-1 α is broadly expressed within the neovascularizing retina, TEAD4 expression is far more limited, restricted to neovascular tufts and a small number of deeper vessels. Therefore, it is possible that antibodies against TEAD4 could be linked to a

cytotoxic conjugate and used for selective elimination of tufts. Similar strategies are currently being tested to deliver cytotoxic taxoid agents for the selective destruction of cancer cells by binding to monoclonal antibodies, polyunsaturated fatty acids, hyaluronic acid, and oligopeptides.⁷³ Wang et al. have demonstrated that Pep-1/IgG conjugates readily cross the plasma membrane of retinal cells *in vivo* following intravitreal injections within mice,⁷⁴ offering a proven vehicle for retinal delivery. Alternatively, selective delivery of the competitive inhibitor TEAD4₂₁₆ to endothelial cells might reduce production of VEGF during neovascularization. The direct contact of the tufts with the vitreous humor would permit delivery of such agents by the relatively common intravitreal injection.

MATERIALS AND METHODS

GENE REPORTER ASSAYS IN YC-1-TREATED MIO-M1

In order to determine the appropriate dosing of YC-1, MIO-M1 cells were seeded at 25K cells per well in 24-well plates filled with 0.5ml DMEM. After 72h, media was replaced with DMEM containing 0, 25, 50, 75, or 100uM YC-1 in DMSO. Cells were moved to a hypoxia chamber flushed with 1%O₂ gas. After 48h, media was taken for measurement of VEGF secretion by ELISA (R&D Systems). Cells were lysed for RNA extraction by RNAqueous and protein by brief sonication in RIPA buffer. Western blotting was performed on pooled hypoxic samples to compare HIF-1 α antibodies from BD Biosciences, Abcam, Santa Cruz, and Cayman Chemical. Western blotting was repeated for the dose response using the Cayman Chemical antibody.

For SEAP reporter assays, MIO-M1 cells were transfected in triplicate with 2.0ug pcDNA.muTEAD1284 and 1.0ug pSEAP.muVEGFproF1R3 by Amaxa electroporation using methods described previously. Media was changed after 24h to DMEM containing

10% FBS with or without 50uM YC-1 in DMSO at a final concentration of 0.5%. Following overnight incubation, media was removed and cells were rapidly harvested in ice-cold RIPA for immediate sonication. Media was assayed for SEAP, and cellular protein was used in Western blotting for TEAD4 and HIF-1 α . This experiment was repeated with electroporated cells split into two plates, one of which was maintained in hypoxia following the media change. Induction of VEGF promoter activity by hypoxia following TEAD4 overexpression was compared with and without YC-1 inhibition of HIF-1 α .

The requirement for HIF-1 α in native VEGF induction was examined by plating 100K MIO-M1 in triplicate in 24-well plates. Media was changed after 24h to fresh DMEM containing 50uM YC-1, 50uM CoCl₂, or DMSO vehicle alone, and cells were placed in hypoxia overnight before harvesting media for VEGF ELISA. Next, the effect of TEAD4 overexpression on native VEGF expression following YC-1 knockdown was examined. Transfections were repeated using 0, 200, or 2000ng of pcDNA.muTEAD1284, with 2000, 1800, and 0 ng of pcDNA.0 respectively. Media was changed after 24h to fresh 10% FBS DMEM containing 0 or 50uM DMSO, with cells moved to hypoxia. Media was harvested for VEGF ELISA 24h later. RNA was purified using RNAqueous kit, reverse transcribed, and assayed for VEGF transcript level by quantitative RT-PCR as described previously.

SEAP REPORTER ASSAYS IN C4 AND 1C1C7 CELLS

C4 and wild-type 1C1C7 cells were grown at 37C in MEM α medium. Cells were plated at a density of 120K cells per well in 24-well plates. Plates were maintained in normal oxygen conditions with 5% CO₂ or in a hypoxic chamber flushed with gas containing 1% O₂ per earlier described protocol. After 24h, cells were sonicated in RIPA for protein analysis or lysed in RNAqueous lysis buffer for total RNA by manufacturer's

protocol. Reverse transcribed cDNA was subject to RT-PCR and qRT-PCR per earlier described protocols, with significance established using Student's two-tailed t-test for $n=3$ with $p<0.05$.

For SEAP gene expression assays, cells were plated at 120K cells/well in 24-well plates. Following an overnight incubation, media was removed, and cells were transfected with 1.0ug of pSEAP reporter plasmid containing the full-length VEGF promoter construct F1R3, along with 2.0ug of each of the four pcDNA3.1 plasmids containing the various TEAD4 isoforms (TEAD4, TEAD4-EX5, TEAD4-YBD, TEAD4-EX5YD) in Lipofectamine 2000 (Invitrogen) and OPTIMEM per manufacturer's protocol.

SIRNA KNOCKDOWN OF HIF-1 α AND TEAD4

MIO-M1 cells were electroporated in triplicate with 50pmol of HIF-1 α siRNA according to previously described protocol. Cells were plated overnight in RPMI1640. Media was changed to DMEM containing 10%FBS at 72h, and cells were in a hypoxia chamber overnight. Cells were harvested at 96h post-electroporation for RNA processing by RNAqueous and sonication in RIPA buffer for protein analysis. For VEGF promoter activity assays, MIO-M1 cells were co-electroporated with 1ug of pSEAP.VEGFproF1R3, 2ug of pcDNA.muTEAD1284 or pcDNA.0 control, and 50pmol of mixed HIF-1 α .siRNA-I and HIF-1 α .siRNA-II. Media was changed following overnight recovery, and cells were maintained for 48h in normoxic or hypoxic conditions. Media was collected and analyzed for SEAP, and cells were sonicated in RIPA for Western blot confirmation of HIF-1 α knockdown and TEAD4 overexpression. Each sample was assayed for SEAP in duplicate by manufacturer's protocol. Significance was established using Student's two-tailed t-test ($n=3$, $p<0.05$).

For evaluation of TEAD4 knockdown, MIO-M1 cells were electroporated in triplicate by the above protocol with 80pmol mixed TEAD4 siRNA. Media was changed after 24h, and cells harvested after 48h, 96h, and 7 days. This was repeated using only 50pmol of each siRNA construct separately to determine relative impact of each. For combined knockdown of HIF-1 α and TEAD4, cells were electroporated with 50pmol of siRNA targeting HIF-1 α or scrambled controls and 80pmol of mixed siRNA targeting TEAD4 or scrambled controls according to previously described protocols. Cells were split to normoxia and hypoxia plates and maintained for 96 hours before harvesting for RNA and protein by the above protocol. Each sample was assayed for *VEGF* transcript level in quadruplicate by quantitative RT-PCR as described previously. Significance was established using Student's two-tailed t-test for n=3 with p<0.05.

IMMUNOHISTOCHEMISTRY

Immunohistochemistry was performed according to published protocol.⁷⁵ Sections from three OIR retinas and three control retinas were thawed at room temperature and incubated in a blocking solution comprised of 3% (v/v) normal horse serum, 0.5% (v/v) Triton X-100, 0.025% (w/v) NaN₃ in PBS for one hour. Slides were washed briefly in three changes of PBS, and then incubated in primary antibodies against TEAD4 (Aviva 38276, 1:500, Aviva Systems Biology) and GLAST (1:500, Chemicon) for one hour. Slides were again washed in three changes of PBS and incubated in secondary antibody (Alexa 546 goat anti-rabbit 1:500) for one hour. FITC-conjugated *Griffonia simplicifolia* isolectin was added to selected secondary incubations. Slides were washed, stained briefly with DAPI, and coverslipped. Visualization was performed using an Olympus Fluoview FV1000 confocal microscope running FV10-ASW software. Exposure was adjusted for each sample in order to prevent saturation of signal. For TEAD4 negative control, Aviva antibody was

preincubated with a 100-fold molar excess of TEAD4 peptide (Aviva). No-primary controls were used for GLAST staining.

Chapter V. SUMMARY AND CONCLUSIONS

TEAD4 INCREASES DURING THE NEOVASCULAR PHASE OF OIR IN THE MOUSE

Previous *in vitro* studies had shown that several endothelial cell types of bovine and human origin upregulated TEAD4 in response to hypoxia, including BAECs, HUVECs, and HMECs.³⁴ However, the level of TEAD4 expression had not previously been quantified in the OIR mouse model. *Tead4* transcription was found to decrease during the vaso-obliterative phase and increase significantly during the neovascular phase of the model, in a pattern correlated to that of *Vegf*. However, there was a lag in increases of *Tead4* when compared to *Vegf*, suggesting that it might not be the causative factor. As Müller glia have been shown to be one of the most important sources of VEGF in the neovascular phase of OIR,¹² their noticeable lack of nuclear TEAD4 expression as observed by IHC limits the potential for involvement of this transcription factor in the progression of neovascularization. However, the human TEAD4₂₁₆ isoform has been shown to inhibit VEGF promoter activity *in vitro*;³⁶ thus it is possible that cytoplasmic TEAD4 may still play a role in VEGF regulation.

THE MIO-M1 CELL LINE HAS A STRONG VEGF TRANSCRIPTIONAL RESPONSE TO HYPOXIA

As the various cell lines were considered for this work, it became obvious that the human Müller glial MIO-M1 line represents a uniquely responsive tool for examining hypoxic response *in vitro*. No other cell line tested had anywhere near the transcriptional response of these cells. It was also shown to be a singular producer of VEGF secretion in

hypoxia. Due to these strong transcriptional responses, this cell line is a logical choice for future research into hypoxic regulation of VEGF expression *in vitro*.

ALL MURINE TEAD4 SPLICE VARIANTS RETAIN A NUCLEAR LOCALIZATION SIGNAL AND ARE CAPABLE OF INCREASING VEGF PROMOTER ACTIVITY

Earlier published data employing native and chimeric human TEAD4 constructs examined what structural features were involved in the regulation of VEGF promoter activity.³⁶ Activator isoforms including TEAD4₄₃₄, TEAD4₃₁₁, and TEAD4₁₄₈ all enhance promoter activity 3-fold to 15-fold above background,³⁶ whereas the inhibitory TEAD4₂₁₆ isoform reduced promoter activity over 20%.³⁶ When fluorescent-protein-tagged versions of these isoforms were overexpressed within HEK293, it was found that all the activator isoforms were localized to the nucleus. However, the inhibitor isoform was retained within the cytoplasm. Gene reporter assays using chimeric constructs showed that the inhibitor isoform could be turned into an activator by the inclusion of the fourth exon containing the NLS from the full-length protein. Further, deletion of the NLS from activator isoforms removed their ability to enhance VEGF promoter activity. The TEAD4 isoforms found within the mouse caused similar strong enhancement of VEGF promoter activity, and this enhancement was consistent with the pattern observed in the human isoforms, as all three variants retained the NLS-containing fourth exon, and all drove similar increases in promoter activity. These data show that similar relationships between regions of the TEAD4 gene hold within murine ocular cells.

TEAD4 KNOCKDOWN REDUCES HIF-1 α EXPRESSION IN A MÜLLER GLIAL

CELL LINE

One of the key questions addressed by this work is whether or not a truly HIF-1 α -independent direct regulation of the VEGF promoter exists. Although HIF-1 α is generally considered to be regulated post-transcriptionally by oxygen-dependent prolyl hydroxylases PHD1, PHD2, and PHD3, the recent work of Jian Li's group has shown that TEAD4 is able to regulate HIF-1 α transcription within BAEC, HUVEC, and HMEC, generating significant changes in the equilibrium level of HIF-1 α protein.⁶² By binding to the second of two MCAT-like sequences in the HIF-1 α promoter, TEAD4 was shown to enhance transcription of HIF-1 α and increase equilibrium protein levels. Their work was performed in various endothelial cell types, but it is quite common for transcription factors to have cell-type-specific behavior. Within the context of the human Müller glial cell line MIO-M1, the evidence presented here suggests that a similar HIF-1 α regulatory pathway operates in this cell type as well. Knockdown of TEAD4 using siRNA reduced levels of HIF-1 α transcription as shown by qRT-PCR and reduced equilibrium protein levels as shown by Western blot. These ocular-derived cells therefore appear to express any cofactors required for TEAD4 to function as a regulator of HIF-1 α .

TEAD4 OVEREXPRESSION OVERCOMES KNOCKDOWN OF HIF-1 α

The work presented here shows that TEAD4 also supports HIF-1 α expression in an ocular-relevant cellular context. Although overexpression of TEAD4 alone did not result in repeatable increases in HIF-1 α in these cells, elevated TEAD4 was able to consistently restore HIF-1 α levels following HIF-1 α knockdown. This suggests that proposed therapeutic strategies to reduce HIF-1 α by chemical inhibitors such as YC-1 may be

ineffective against hypoxia-driven neovascularization due to the ability of TEAD4 to overcome HIF-1 α inhibition.

TEAD4 KNOCKDOWN REDUCES VEGF EXPRESSION BY A HIF-1A-DEPENDENT INDIRECT PATHWAY

When the finding that HIF-1 α was regulated by TEAD4 was published, much of the data presented here were re-examined in light of the impact of TEAD4 on HIF-1 α . The assumption that the effect of TEAD4 on VEGF expression was secondary to its impact on HIF-1 α explained the seemingly conflicting outcomes of our early investigations into HIF independence. Although results that supported a role for the direct regulation of VEGF by TEAD4 using YC-1 were initially at odds with those using siRNA knockdown of HIF-1 α , examination of HIF-1 α levels showed that the effect could be explained by restoration of HIF-1 α levels driven by TEAD4 overexpression. The evidence from promoter assays incorporating HRE-deleted constructs, as well as the native *VEGF* expression patterns following various combinations of HIF-1 α and TEAD4 knockdown, indicate that the hypoxic induction of *VEGF* expression is likely due to the indirect effect of TEAD4 on HIF-1 α transcriptional regulation. Thus, we conclude that increases in VEGF transcription under hypoxia following TEAD4 overexpression are an indirect consequence of the ability of TEAD4 to drive HIF-1 α expression.

TEAD4 EXPRESSION IS HIGH WITHIN RETINAL VASCULAR ENDOTHELIAL CELLS OF NEOVASCULAR TUFTS

The finding that endothelial cells within preretinal tufts of the OIR retina express high levels of TEAD4 is intriguing given that multiple EC types have been shown to upregulate TEAD4 under hypoxia *in vitro*, and TEAD4 involvement in the hypoxic response of ocular

ECs in the murine retina would represent a logical extension of this behavior. Given the knowledge that overexpression of TEAD4 in ECs increases HIF-1 α expression, strategies such as siRNA or cytotoxin-antibody conjugates targeting TEAD4 might be able to effectively reduce the neovascular response within hypoxic retinal diseases such as ROP, DR, and exudative AMD. The relatively easy access to preretinal tufts by way of intravitreal injection makes this an attractive therapeutic approach for future investigation, and Wang et al. have demonstrated that the Pep1 transfection reagent is able to readily deliver complexes to cells of the retinal surface following intravitreal injection.⁷⁴

THE OXYGEN-INDUCED RETINOPATHY MOUSE MODEL IS LIKELY TO OFFER USEFUL INSIGHT INTO TEAD4 INTERACTIONS WITH VEGF

In addition to the widespread interest in the OIR model of neovascularization, another goal of this work was to determine whether or not the mouse model of OIR would be a suitable platform to investigate interactions of TEAD4 with the VEGF promoter *in vivo*. In order for studies within the mouse to have predictive value for the behavior within human disease, it is necessary to see similar behavior when comparing the mouse and human promoters. The results presented here demonstrate little difference between the activity enhancements observed for the human and mouse promoters, which supports the use of the OIR model for investigation of TEAD4 interactions with HIF-1 α and VEGF in human neovascular diseases.

It is of particular interest to determine whether or not the recently reported inhibitory TEAD4₂₁₆ isoform is capable of competitively inhibiting activator isoforms that are involved in the progression of retinopathies. In that study, overexpression of the inhibitor isoform was capable of reducing TEAD4 promoter activity even when co-transfected with activator

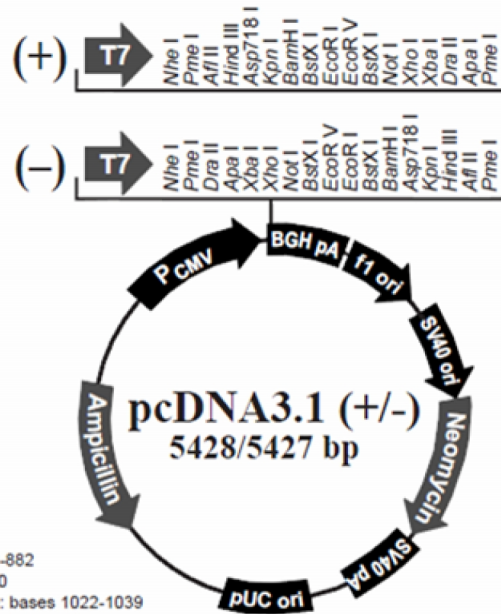
isoforms such as TEAD4₁₄₈.³⁶ Given the findings here that TEAD4 is overexpressed within ECs of neovascular tufts, it is possible that this transcription factor may be involved in the generation of these pathological features. Consequently, delivery of the inhibitor isoform to examine the impact on neovascularization *in vivo* would likely be a worthwhile experimental pursuit.

FUTURE DIRECTIONS

Since Li et al. worked strictly with the full-length isoform of TEAD4, it would be interesting to investigate whether or not the other TEAD4 isoforms differ in their ability to drive HIF-1 α . Since the TEAD4₂₁₆ isoform was shown to competitively inhibit VEGF promoter activity, it would be particularly interesting to know if this recently published variant was capable of competitively inhibiting HIF-1 α levels. As this pathway was not explored, it would enhance our understanding of the role of TEAD4 isoforms in HIF-1 α promoter regulation, with potential implications for therapeutic intervention strategies in retinopathies as well as anti-angiogenic oncology strategies.

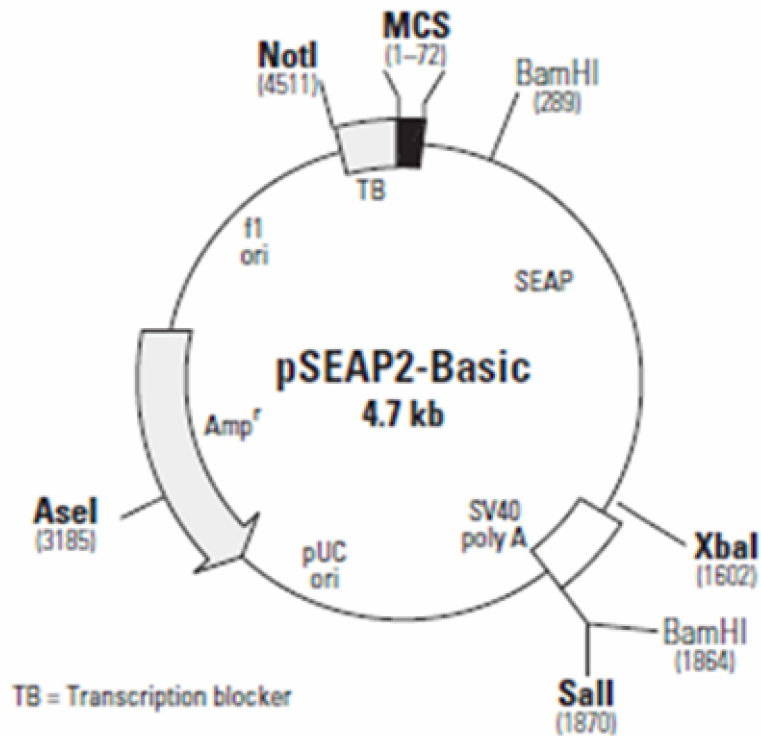
Given the findings regarding EC expression of TEAD4 in the OIR model, it might be worthwhile to spend additional effort in pursuit of modeling TEAD4/HIF-1 α /VEGF interactions in hypoxia using ocular ECs from other sources. While RF/6A cells were examined briefly in this work, the focus of effort was limited to Müller glia in the interest of time. Other sources of ocular ECs, including acutely dissociated primary cell cultures, might yield greater insight into the interactions of TEAD4 with HIF-1 α and VEGF transcription *in vivo*. As noted above, these studies could yield new therapies for treatment of human neovascular diseases.

APPENDIX A



Comments for pcDNA3.1 (+)
5428 nucleotides

- CMV promoter: bases 232-819
- T7 promoter/priming site: bases 863-882
- Multiple cloning site: bases 895-1010
- pcDNA3.1/BGH reverse priming site: bases 1022-1039
- BGH polyadenylation sequence: bases 1028-1252
- f1 origin: bases 1298-1726
- SV40 early promoter and origin: bases 1731-2074
- Neomycin resistance gene (ORF): bases 2136-2930
- SV40 early polyadenylation signal: bases 3104-3234
- pUC origin: bases 3617-4287 (complementary strand)
- Ampicillin resistance gene (*bla*): bases 4432-5428 (complementary strand)
- ORF: bases 4432-5292 (complementary strand)
- Ribosome binding site: bases 5300-5304 (complementary strand)
- bla* promoter (P3): bases 5327-5333 (complementary strand)



REFERENCES

- ¹ Penn JS, Madan A, Caldwell RB, Bartoli M, Caldwell RW, Hartnett ME. Vascular endothelial growth factor in eye disease. *Prog Retin Eye Res.* 2008 Jul;27(4):331-71. doi: 10.1016/j.preteyeres.2008.05.001. Epub 2008 May 28. Review. PubMed PMID: 18653375.
- ² Palmer EA, Flynn JT, Hardy RJ, Phelps DL, Phillips CL, Schaffer DB, Tung B. Incidence and early course of retinopathy of prematurity. The Cryotherapy for Retinopathy of Prematurity Cooperative Group. *Ophthalmology.* 1991 Nov;98(11):1628-40. PubMed PMID: 1800923.
- ³ Steinkuller PG, Du L, Gilbert C, Foster A, Collins ML, Coats DK. Childhood blindness. *J AAPOS.* 1999 Feb;3(1):26-32. PubMed PMID: 10071898.
- ⁴ Sears NC, Sears JE. Oxygen and retinopathy of prematurity. *Int Ophthalmol Clin.* 2011 Winter;51(1):17-31. doi: 10.1097/IIO.0b013e3182009916. Review. PubMed PMID: 21139475.
- ⁵ Law JC, Recchia FM, Morrison DG, Donahue SP, Estes RL. Intravitreal bevacizumab as adjunctive treatment for retinopathy of prematurity. *J AAPOS.* 2010 Feb;14(1):6-10. doi: 10.1016/j.jaapos.2009.10.011. PubMed PMID: 20227614.
- ⁶ Mititelu M, Chaudhary KM, Lieberman RM. An Evidence-Based Meta-analysis of Vascular Endothelial Growth Factor Inhibition in Pediatric Retinal Diseases: Part 1. Retinopathy of Prematurity. *J Pediatr Ophthalmol Strabismus.* 2012 Aug 28;1-9. doi: 10.3928/01913913-20120821-03. [Epub ahead of print] PubMed PMID: 22938516.
- ⁷ Update on Anti-VEGF Monotherapy for ROP. Franco M. Recchia, MD, Nashville, Tenn., Antonio Capone Jr., MD, Royal Oak, Mich. Review of *Ophthalmology Online.* 8/15/2011
- ⁸ Ashton N, Blach R. STUDIES ON DEVELOPING RETINAL VESSELS VIII. EFFECT OF OXYGEN ON THE RETINAL VESSELS OF THE RATLING. *Br J Ophthalmol.* 1961 May;45(5):321-40. PubMed PMID: 18170681; PubMed Central PMCID: PMC510085.
- ⁹ Ashton N, Tripathi B, Knight G. Effect of oxygen on the developing retinal vessels of the rabbit. I. Anatomy and development of the retinal vessels of the rabbit. *Exp Eye Res.* 1972 Nov;14(3):214-20. PubMed PMID: 4640870.
- ¹⁰ Kremer I, Kissun R, Nissenkorn I, Ben-Sira I, Garner A. Oxygen-induced retinopathy in newborn kittens. A model for ischemic vasoproliferative retinopathy. *Invest Ophthalmol Vis Sci.* 1987 Jan;28(1):126-30. PubMed PMID:2433248.
- ¹¹ Smith LE, Wesolowski E, McLellan A, et al. Oxygen-induced retinopathy in the mouse. *Invest Ophthalmol Vis Sci.* 1994;35:101-111.
- ¹² Pierce EA, Avery RL, Foley ED, Aiello LP, Smith LE. Vascular endothelial growth factor/vascular permeability factor expression in a mouse model of retinal neovascularization. *Proc Natl Acad Sci U S A.* 1995 Jan 31;92(3):905-9. PubMed PMID: 7846076; PubMed Central PMCID: PMC42729.
- ¹³ Holmes DI, Zachary I. The vascular endothelial growth factor (VEGF) family: angiogenic factors in health and disease. *Genome Biol.* 2005;6(2):209.
- ¹⁴ Matsumoto T, Claesson-Welsh L. VEGF receptor signal transduction. *Sci STKE.* 2001 Dec 11;2001(112):re21. Review. PubMed PMID: 11741095.
- ¹⁵ Zhang F, Tang Z, Hou X, Lennartsson J, Li Y, Koch AW, Scotney P, Lee C, Arjunan P, Dong L, Kumar A, Rissanen TT, Wang B, Nagai N, Fons P, Fariss R, Zhang Y, Wawrousek E, Tansey G, Raber J, Fong GH, Ding H, Greenberg DA, Becker KG, Herbert JM, Nash A, Yla-Herttuala S, Cao Y, Watts RJ, Li X. VEGF-B is dispensable for blood vessel growth but critical for their survival, and VEGF-B targeting inhibits pathological angiogenesis. *Proc Natl Acad Sci U S A.* 2009 Apr 14;106(15):6152-7. doi: 10.1073/pnas.0813061106. Epub 2009 Apr 6. PubMed PMID: 19369214; PubMed Central PMCID: PMC2669337.

-
- ¹⁶ Hagberg CE, Falkevall A, Wang X, Larsson E, Huusko J, Nilsson I, van Meeteren LA, Samen E, Lu L, Vanwildemeersch M, Klar J, Genove G, Pietras K, Stone-Elander S, Claesson-Welsh L, Ylä-Herttuala S, Lindahl P, Eriksson U. Vascular endothelial growth factor B controls endothelial fatty acid uptake. *Nature*. 2010 Apr 8;464(7290):917-21. doi: 10.1038/nature08945. Epub 2010 Mar 14. PubMed PMID: 20228789.
- ¹⁷ Forsythe JA, Jiang BH, Iyer NV, Agani F, Leung SW, et al. (1996) Activation of vascular endothelial growth factor gene transcription by hypoxia-inducible factor 1. *Mol Cell Biol* 16: 4604–4613.
- ¹⁸ Tischer E, Mitchell R, Hartman T, Silva M, Gospodarowicz D, Fiddes JC, Abraham JA. The human gene for vascular endothelial growth factor. Multiple protein forms are encoded through alternative exon splicing. *J Biol Chem*. 1991 Jun 25;266(18):11947-54. PubMed PMID: 1711045.
- ¹⁹ Garrido C, Saule S, Gospodarowicz D. Transcriptional regulation of vascular endothelial growth factor gene expression in ovarian bovine granulosa cells. *Growth Factors*. 1993;8(2):109-17. PubMed PMID: 8466753.
- ²⁰ Shima DT, Kuroki M, Deutsch U, Ng YS, Adamis AP, D'Amore PA. The mouse gene for vascular endothelial growth factor. Genomic structure, definition of the transcriptional unit, and characterization of transcriptional and post-transcriptional regulatory sequences. *J Biol Chem*. 1996 Feb 16;271(7):3877-83. PubMed PMID: 8632007.
- ²¹ Dibbens, J. A., Miller, D. L., Damert, A., Risau, W., Vadas, M. A. and Goodall, G. J. (1999). Hypoxic regulation of vascular endothelial growth factor mRNA stability requires the cooperation of multiple RNA elements. *Mol. Biol. Cell*. 10, 907-919.
- ²² Harper SJ, Bates DO. VEGF-A splicing: the key to anti-angiogenic therapeutics? *Nat Rev Cancer*. 2008 Nov;8(11):880-7. doi: 10.1038/nrc2505. Epub 2008 Oct 16. Review. PubMed PMID: 18923433; PubMed Central PMCID: PMC2613352.
- ²⁴ O'Rourke JF, Dachs GU, Gleadle JM, Maxwell PH, Pugh CW, Stratford IJ, Wood SM, Ratcliffe PJ. Hypoxia response elements. *Oncol Res*. 1997;9(6-7):327-32. Review. PubMed PMID: 9406238.
- ²⁵ Wenger RH, Stiehl DP, Camenisch G. Integration of oxygen signaling at the consensus HRE. *Sci STKE*. 2005 Oct 18;2005(306):re12. Review. PubMed PMID: 16234508.
- ²⁶ Maxwell PH, Wiesener MS, Chang GW, Clifford SC, Vaux EC, Cockman ME, Wykoff CC, Pugh CW, Maher ER, Ratcliffe PJ. The tumour suppressor protein VHL targets hypoxia-inducible factors for oxygen-dependent proteolysis. *Nature*. 1999 May 20;399(6733):271-5.
- ²⁷ Wang GL, Semenza GL. Characterization of hypoxia-inducible factor 1 and regulation of DNA binding activity by hypoxia. *J Biol Chem*. 1993 Oct 15;268(29):21513-8. PubMed PMID: 8408001.
- ²⁸ Arany Z, Huang LE, Eckner R, Bhattacharya S, Jiang C, Goldberg MA, Bunn HF, Livingston DM. An essential role for p300/CBP in the cellular response to hypoxia. *Proc Natl Acad Sci U S A*. 1996 Nov 12;93(23):12969-73. PubMed PMID:8917528; PubMed Central PMCID: PMC24030.
- ²⁹ Bringmann A, Pannicke T, Grosche J, Francke M, Wiedemann P, Skatchkov SN, Osborne NN, Reichenbach A. Müller cells in the healthy and diseased retina. *Prog Retin Eye Res*. 2006 Jul;25(4):397-424. Epub 2006 Jul 12. Review. PubMed PMID:16839797.
- ³⁰ García M, Vecino E. Role of Müller glia in neuroprotection and regeneration in the retina. *Histol Histopathol*. 2003 Oct;18(4):1205-18. Review. PubMed PMID:12973689.
- ³¹ Cajal SR. In: Thorpe SA, Glickstein M, translators. 1892. *The structure of the retina*. Springfield (IL): Thomas; 1972.
- ³² Lin M, Chen Y, Jin J, Hu Y, Zhou KK, Zhu M, Le YZ, Ge J, Johnson RS, Ma JX. Ischaemia-induced retinal neovascularisation and diabetic retinopathy in mice with conditional knockout of hypoxia-inducible factor-1 in retinal Müller cells. *Diabetologia*. 2011 Jun;54(6):1554-66. doi: 10.1007/s00125-011-2081-0. Epub 2011 Mar 1. PubMed PMID: 21360191.

-
- ³³ Bai Y, Ma JX, Guo J, Wang J, Zhu M, Chen Y, Le YZ. Müller cell-derived VEGF is a significant contributor to retinal neovascularization. *J Pathol.* 2009 Dec;219(4):446-54. doi: 10.1002/path.2611. PubMed PMID: 19768732.
- ³⁴ Jue-Lon Shie, Guifu Wu, Jiaping Wu, Fen-Fen Liu, Roger J. Laham, Peter Oettgen, and Jian Li RTEF-1, a Novel Transcriptional Stimulator of Vascular Endothelial Growth Factor in Hypoxic Endothelial Cells*
- ³⁵ Appukuttan B, McFarland TJ, Davies MH, Atchaneeyasakul LO, Zhang Y, et al. (2007) Identification of novel alternatively spliced isoforms of RTEF-1 within human ocular vascular endothelial cells and murine retina. *Invest Ophthalmol Vis Sci* 48: 3775–3782.
- ³⁶ Appukuttan B, McFarland TJ, Stempel A, Kassem JB, Hartzell M, Zhang Y, Bond D, West K, Wilson R, Stout A, Pan Y, Ilias H, Robertson K, Klein ML, Wilson D, Smith JR, Stout JT. The related transcriptional enhancer factor-1 isoform, TEAD4(216), can repress vascular endothelial growth factor expression in mammalian cells. *PLoS One.* 2012;7(6):e31260. Epub 2012 Jun 22.
- ³⁷ Davidson I, Xiao JH, Rosales R, Staub A, Chambon P. The HeLa cell protein TEF-1 binds specifically and cooperatively to two SV40 enhancer motifs of unrelated sequence. *Cell.* 1988 Sep 23;54(7):931-42.
- ³⁸ Shimizu N, Dizon E, Zak R. Both muscle-specific and ubiquitous nuclear factors are required for muscle-specific expression of the myosin heavy-chain beta gene in cultured cells. *Mol Cell Biol.* 1992 Feb;12(2):619-30. PubMed PMID: 1732734.
- ³⁹ Stewart AF, Richard CW 3rd, Suzow J, Stephan D, Weremowicz S, Morton CC, Adra CN. Cloning of human RTEF-1, a transcriptional enhancer factor-1-related gene preferentially expressed in skeletal muscle: evidence for an ancient multigene family. *Genomics.* 1996 Oct 1;37(1):68-76.
- ⁴⁰ Yockey CE, Smith G, Izumo S, Shimizu N. cDNA cloning and characterization of murine transcriptional enhancer factor-1-related protein 1, a transcription factor that binds to the M-CAT motif. *J Biol Chem.* 1996 Feb 16;271(7):3727-36.
- ⁴¹ Yasunami M, Suzuki K, Ohkubo H. A novel family of TEA domain-containing transcription factors with distinct spatiotemporal expression patterns. *Biochem Biophys Res Commun.* 1996 Nov 12;228(2):365-70.
- ⁴² Stewart AF, Suzow J, Kubota T, Ueyama T, Chen HH. Transcription factor RTEF-1 mediates alpha1-adrenergic reactivation of the fetal gene program in cardiac myocytes. *Circ Res.* 1998 Jul 13;83(1):43-9.
- ⁴³ Xiao JH, Davidson I, Matthes H, Garnier JM, Chambon P. Cloning, expression, and transcriptional properties of the human enhancer factor TEF-1. *Cell.* 1991 May 17;65(4):551-68.
- ⁴⁴ Farrance IK, Mar JH, Ordahl CP. M-CAT binding factor is related to the SV40 enhancer binding factor, TEF-1. *J Biol Chem.* 1992 Aug 25;267(24):17234-40. PubMed PMID: 1324927.
- ⁴⁵ Blatt C, DePamphilis ML. Striking homology between mouse and human transcription enhancer factor-1 (TEF-1). *Nucleic Acids Res.* 1993 Feb 11;21(3):747-8. PubMed PMID: 8441689; PubMed Central PMCID: PMC309183.
- ⁴⁶ Burglin, T.R. (1991) *Cell*, 66, 11-12.
- ⁴⁷ Hwang JJ, Chambon P, Davidson I. Characterization of the transcription activation function and the DNA binding domain of transcriptional enhancer factor-1. *EMBO J.* 1993 Jun;12(6):2337-48. PubMed PMID: 8389695; PubMed Central PMCID: PMC413464.
- ⁴⁸ Yasunami M, Suzuki K, Houtani T, Sugimoto T, Ohkubo H. Molecular characterization of cDNA encoding a novel protein related to transcriptional enhancer factor-1 from neural precursor cells. *J Biol Chem.* 1995 Aug 4;270(31):18649-54. PubMed PMID: 7629195.
- ⁴⁹ Milewski RC, Chi NC, Li J, Brown C, Lu MM, Epstein JA. Identification of minimal enhancer elements sufficient for Pax3 expression in neural crest and implication of Tead2 as a regulator of Pax3. *Development.* 2004 Feb;131(4):829-37. Epub 2004 Jan 21. Erratum in: *Development.* 2004 Mar;131(5):1195. PubMed PMID:14736747.

-
- ⁵⁰ Azakie A, Larkin SB, Farrance IK, Grenningloh G, Ordahl CP. DTEF-1, a novel member of the transcription enhancer factor-1 (TEF-1) multigene family. *J Biol Chem*. 1996 Apr 5;271(14):8260-5. PubMed PMID: 8626520.
- ⁵¹ Yockey CE, Shimizu N. cDNA cloning and characterization of mouse DTEF-1 and ETF, members of the TEA/ATTS family of transcription factors. *DNA Cell Biol*. 1998 Feb;17(2):187-96. PubMed PMID: 9502435.
- ⁵² Jacquemin P, Martial JA, Davidson I. Human TEF-5 is preferentially expressed in placenta and binds to multiple functional elements of the human chorionic somatomammotropin-B gene enhancer. *J Biol Chem*. 1997 May 16;272(20):12928-37. PubMed PMID: 9148898.
- ⁵³ Ueyama T, Zhu C, Valenzuela YM, Suzow JG, Stewart AF. Identification of the functional domain in the transcription factor RTEF-1 that mediates alpha1-adrenergic signaling in hypertrophied cardiac myocytes. *J Biol Chem*. 2000 Jun 9;275(23):17476-80. PubMed PMID: 10764782.
- ⁵⁴ Anbanandam A, Albarado DC, Nguyen CT, Halder G, Gao X, Veeraraghavan S. Insights into transcription enhancer factor 1 (TEF-1) activity from the solution structure of the TEA domain. *Proc Natl Acad Sci U S A*. 2006 Nov 14;103(46):17225-30. Epub 2006 Nov 3. PubMed PMID: 17085591; PubMed Central PMCID: PMC1859914.
- ⁵⁵ Vassilev A, Kaneko KJ, Shu H, Zhao Y, DePamphilis ML. TEAD/TEF transcription factors utilize the activation domain of YAP65, a Src/Yes-associated protein localized in the cytoplasm. *Genes Dev*. 2001 May 15;15(10):1229-41. PubMed PMID: 11358867; PubMed Central PMCID: PMC313800.
- ⁵⁶ Mahoney WM Jr, Hong JH, Yaffe MB, Farrance IK. The transcriptional co-activator TAZ interacts differentially with transcriptional enhancer factor-1 (TEF-1) family members. *Biochem J*. 2005 May 15;388(Pt 1):217-25. PubMed PMID: 15628970; PubMed Central PMCID: PMC1186710.
- ⁵⁷ Zhang L, Ren F, Zhang Q, Chen Y, Wang B, Jiang J. The TEAD/TEF family of transcription factor Scalloped mediates Hippo signaling in organ size control. *Dev Cell*. 2008 Mar;14(3):377-87. Epub 2008 Feb 7. PubMed PMID: 18258485; PubMed Central PMCID: PMC2292673.
- ⁵⁸ Zhao B, Ye X, Yu J, Li L, Li W, Li S, Yu J, Lin JD, Wang CY, Chinnaiyan AM, Lai ZC, Guan KL. TEAD mediates YAP-dependent gene induction and growth control. *Genes Dev*. 2008 Jul 15;22(14):1962-71. Epub 2008 Jun 25. PubMed PMID: 18579750; PubMed Central PMCID: PMC2492741.
- ⁵⁹ Li Z, Zhao B, Wang P, Chen F, Dong Z, Yang H, Guan KL, Xu Y. Structural insights into the YAP and TEAD complex. *Genes Dev*. 2010 Feb 1;24(3):235-40. PubMed PMID: 20123905; PubMed Central PMCID: PMC2811825.
- ⁶⁰ Chen L, Chan SW, Zhang X, Walsh M, Lim CJ, Hong W, Song H. Structural basis of YAP recognition by TEAD4 in the hippo pathway. *Genes Dev*. 2010 Feb 1;24(3):290-300. PubMed PMID: 20123908; PubMed Central PMCID: PMC2811830.
- ⁶¹ Liu-Chittenden Y, Huang B, Shim JS, Chen Q, Lee SJ, Anders RA, Liu JO, Pan D. Genetic and pharmacological disruption of the TEAD-YAP complex suppresses the oncogenic activity of YAP. *Genes Dev*. 2012 Jun 15;26(12):1300-5. Epub 2012 Jun 7. PubMed PMID: 22677547; PubMed Central PMCID: PMC3387657.
- ⁶² Jin Y, Wu J, Song X, Song Q, Cully BL, Messmer-Blust A, Xu M, Foo SY, Rosenzweig A, Li J. RTEF-1, an upstream gene of hypoxia-inducible factor-1 α , accelerates recovery from ischemia. *J Biol Chem*. 2011 Jun 24;286(25):22699-705.
- ⁶³ Jiang SW, Trujillo MA, Sakagashira M, Wilke RA, Eberhardt NL. Novel human TEF-1 isoforms exhibit altered DNA binding and functional properties. *Biochemistry*. 2000 Mar 28;39(12):3505-13. PubMed PMID: 10727247.
- ⁶⁴ Davies MH, Eubanks JP, Powers MR. Increased retinal neovascularization in Fas ligand-deficient mice. *Invest Ophthalmol Vis Sci*. 2003;44:3202-3210.
- ⁶⁵ Otteson DC, Phillips MJ. A conditional immortalized mouse Müller glial cell line expressing glial and retinal stem cell genes. *Invest Ophthalmol Vis Sci*. 2010 Nov;51(11):5991-6000.

-
- ⁶⁶ Limb GA, Salt TE, Munro PM, Moss SE, Khaw PT. In vitro characterization of a spontaneously immortalized human Müller cell line (MIO-M1). *Invest Ophthalmol Vis Sci.* 2002 Mar;43(3):864-9. PubMed PMID: 11867609.
- ⁶⁷ Liu Y, Cox SR, Morita T, Kourembanas S. Hypoxia regulates vascular endothelial growth factor gene expression in endothelial cells. Identification of a 5' enhancer. *Circ Res.* 1995 Sep;77(3):638-43.
- ⁶⁸ Minchenko A, Salceda S, Bauer T, Caro J. Hypoxia regulatory elements of the human vascular endothelial growth factor gene. *Cell Mol Biol Res.* 1994;40(1):35-9.
- ⁶⁹ Levy AP, Levy NS, Wegner S, Goldberg MA. Transcriptional regulation of the rat vascular endothelial growth factor gene by hypoxia. *J Biol Chem.* 1995 Jun 2;270(22):13333-40.
- ⁷⁰ DeNiro M, Al-Halafi A, Al-Mohanna FH, Alsmadi O, Al-Mohanna FA. Pleiotropic effects of YC-1 selectively inhibit pathological retinal neovascularization and promote physiological revascularization in a mouse model of oxygen-induced retinopathy. *Mol Pharmacol.* 2010 Mar;77(3):348-67.
- ⁷¹ Wang J, Xu X, Elliott MH, Zhu M, Le YZ. Müller cell-derived VEGF is essential for diabetes-induced retinal inflammation and vascular leakage. *Diabetes.* 2010 Sep;59(9):2297-305. doi: 10.2337/db09-1420. Epub 2010 Jun 8. PubMed PMID:20530741; PubMed Central PMCID: PMC2927953.
- ⁷² Appukuttan B, McFarland TJ, Stempel A, Kassem JB, Hartzell M, Zhang Y, Bond D, West K, Wilson R, Stout A, Pan Y, Ilias H, Robertson K, Klein ML, Wilson D, Smith JR, Stout JT. The related transcriptional enhancer factor-1 isoform, TEAD4(216), can repress vascular endothelial growth factor expression in mammalian cells. *PLoS One.* 2012;7(6):e31260. doi: 10.1371/journal.pone.0031260. Epub 2012 Jun 22. PubMed PMID: 22761647; PubMed Central PMCID: PMC3382240.
- ⁷³ Chen J, Jaracz S, Zhao X, Chen S, Ojima I. Antibody-cytotoxic agent conjugates for cancer therapy. *Expert Opin Drug Deliv.* 2005 Sep;2(5):873-90.
- ⁷⁴ Wang MH, Frishman LJ, Otteson DC. Intracellular delivery of proteins into mouse Müller glia cells in vitro and in vivo using Pep-1 transfection reagent. *J Neurosci Methods.* 2009 Mar 15;177(2):403-19.
- ⁷⁵ Morgans CW, Ren G, Akileswaran L. Localization of nyctalopin in the mammalian retina. *Eur J Neurosci* 2006; 23:1163–1171.